Journal of Revenue and Pricing Management (2025) 24:153–177
https://doi.org/10.1057/s41272-024-00478-6

RESEARCH ARTICLE

Modeling price-sensitive demand in turbulent times: an application to continuous pricing

Felix Meyer[1] · Göran Kauermann[1] · Christopher Alder[2] · Catherine Cleophas[3]

Received: 4 July 2023 / Accepted: 21 December 2023 / Published online: 28 July 2024

Abstract

Pricing drives demand for service industries such as air transport, hotels, and car rentals. To optimise the price, firms have to predict real-time customer demand at the micro level and optimise the price. This paper contributes to revenue management by introducing a nonparametric statistical approach to predict price-sensitive demand and its application to continuous pricing. Continuous pricing lets service companies maximise revenue by using customers' willingness to pay. However, it requires accurate demand estimations, particularly of customers' price sensitivity. This paper introduces an augmented generalised additive model to estimate price sensitivity, which identifies substantial variations in price sensitivity, exceeds the predictive performance of state-of-the-art alternatives, and controls for price endogeneity. In addition, the demand model has variable price derivatives enabling continuous pricing. The proposed approach offers a simple and efficient way to implement continuous pricing with a closed-form solution. Our research also highlights the relevance of considering the problem of price endogeneity when estimating price-sensitive demand based on observations from prior pricing decisions. We demonstrate how continuous pricing is applied using empirical airline ticket data. We document a field study, which shows a revenue increase of 6% on average, and outline how the approach applies to turbulent market conditions caused by the COVID-19 pandemic, the surge in inflation since mid-2021, and the start of the Ukraine war in April 2022.

Keywords Price-sensitivity · Dynamic pricing · Nonparametric demand forecasting · Poisson process · Price endogeneity · Revenue management · COVID-19 · Turbulent market conditions

Introduction

Airlines want to reduce distribution costs and increase control of the offered content (Bingemer 2018). In doing so airlines have focused on revolutionizing how their products are retailed and distributed (IATA 2018). From the passengers' point of view, the airline initiative leads to a new shopping experience with more personalized offers (Wittman and Belobaba 2017), increased accuracy in pricing (Wittman and Belobaba 2019), and more convenient customer touch points (Sankaranarayanan and Lalchandani 2019) to sell new and customized products.

For airlines to leverage the newfound flexibility to increase their profitability, changes to the revenue management methodology (such as continuous pricing) are required that can quickly adopted in practice. Particularly, the past years highlight the airline's need to quickly adapt to changing market conditions. Since the beginning of

✉ Felix Meyer
fm1000@gmx.de
https://www.wisostat.statistik.uni-muenchen.de

Göran Kauermann
goeran.kauermann@stat.uni-muenchen.de
https://www.wisostat.statistik.uni-muenchen.de

Christopher Alder
christopher.alder@dlh.de

Catherine Cleophas
cleophas@bwl.uni-kiel.de

[1] Department of Statistics, Ludwigs-Maximilians-Universität München, Ludwigstraße 33, 80539 Munich, Germany

[2] Lufthansa Group, Revenue Management, Munich-Airport, Nordallee 25, 85356 Munich, Germany

[3] Institute of Business, Christian-Albrechts Universität zu Kiel, Olshausenstrasse 40, 24118 Kiel, Germany

2020, the global COVID-19 pandemic has led to an unprecedented crisis in the global aviation industry. In mid-2021, the rapid surge in inflation caused huge concerns for the global economy. Most recently, the Ukraine war in April 2022 and the Isreal-Hamas-war in 2023 have added additional complexity and uncertainty to the market. These events underscore the need for alternative approaches and careful consideration when analyzing current market conditions. From an airline operations perspective, all the revenue management systems depending on demand-forecasting models for price optimization need to be corrected as they rely on data recorded before the start of market turbulences.

This paper demonstrates to airline managers a method to optimize revenue in a discrete (booking class-based) and continuous pricing context that can be easily applied using a closed-form optimal pricing solution. Given that the proposed methodology offers unique insights into how passenger demand and price elasticity change by analyzing data gathered during turbulent times, such as the COVID-19 pandemic, it shows airline practitioners how their pricing can be controlled during turbulent market conditions. Finally, the paper shares a large field study with airline practitioners, showing how the proposed method performed in a real-world environment and its ability to increase revenue by 6% on average.

From a technical point of view, our work contributes to the literature on service demand estimation and pricing by extending the class of nonparametric models by augmenting the generalised additive model framework (e.g. Wood 2017), combined with monotonicity constraints (Pya and Wood 2014) and ANOVA type interactions (Lee and Durbán 2011), which also corrects for price endogeneity. Considering competing approaches, which include the parametric model of Fiig et al. (2014), the nonparametric model of Vulcano et al. (2012), and the heuristic of Weatherford and Pölt (2002), we show that our approach yields superior forecasting accuracy using empirical airline data.

In the remainder of this paper, "Literature review on demand estimation and dynamic pricing" section reviews related literature on demand estimation and dynamic pricing. "Statistical model and estimation" section outlines the model. "Empirical data" section discusses applying the model to empirical airline data. "Dynamic pricing" section presents a dynamic pricing algorithm. The practical applicability of our approach within the airline industry is highlighted within "Dynamic pricing" section. Finally, "Conclusion" section concludes the paper.

Literature review on demand estimation and dynamic pricing

The literature on demand estimation given functional structures can be categorised into two groups. The first group includes parametric and linear models, which implicitly assume constant price sensitivity. An example is the parametric, multiplicative, and non-linear forecast model (FCST) of Fiig et al. (2014). In FCST, the upsell probability captures price sensitivity and is assumed to be independent of other confounders. To model a customer choice, multinomial logit (MNL) models are proposed by Vulcano et al. (2010), Newman et al. (2014), Dai et al. (2014), and Xie et al. (2016). All these approaches assume a linear relationship between covariates and the utility defining the choice probability.

The second group represents nonparametric techniques that allow for more complex concepts of price sensitivity. Relaxing the linearity assumption, Vulcano et al. (2012) introduces a nonparametric approach based on the expectation maximisation (EM) algorithm. They employ a mixture of a Poisson- and MNL distribution, where a multinomial utility choice model links the booking decision to a choice probability. The model also differentiates primary and secondary demand, i.e., assuming customers' first choice to be available.

Similar to related work of Arandia (2013) and Wu and Akbarov (2012), we model customer arrivals by a nonhomogeneous Poisson process (NHPP). Thus, the Poisson intensity defines the expected number of arrivals per day. The Poisson intensity is modelled as a function of covariates and accounts for variable price sensitivity. Already, several contributions focus on NHPP and propose data-driven techniques to capture a dynamic arrival rate while abandoning pre-defined functional structures. To model the NHPP's cumulative intensity function nonparametrically, Leemis (1991) proposes piecewise-linear interpolation. Zhang and Kou (2010) analyse the doubly stochastic Poisson process (or Cox process) and show that nonparametric kernel functions improve the fit for high arrival rates. Beyond parametric or nonparametric demand functions, heuristics use imputation when demand observations are censored. In revenue management, this challenge arises when the product is not offered during part of the sales horizon. In such situations, Weatherford and Pölt (2002) proposed substituting demand with the mean number of bookings.

The (dynamic) pricing literature also discusses parametric versus nonparametric demand estimation approaches. Given Poisson-distributed customer arrivals, where a Bernoulli variable defines the purchase probability, Avramidis (2013) proposes a way to estimate arrival

rates and purchase probabilities. The authors show their approach can outperform the estimator introduced in Besbes and Zeevi (2009). Given a linear demand-price relationship, Keskin and Zeevi (2014) proposes the greedy iterative least squares (GILS) approach. Extending this work, Besbes and Zeevi (2015) shows that assuming a linear price-demand relationship does not significantly diminish revenue under reasonably general conditions. Including additional covariates such as market expenditures, geographical information, and socio-economic attributes, Qiang and Bayati (2016) extend the GILS approach. Also, assuming linearity for every covariate, the authors show asymptotically optimal performance.

Abandoning the linearity assumption, Farias et al. (2013) captures customers' choice behaviour to predict revenue gains. The authors conclude that nonparametric techniques are better suited for large-scale automatization as they rely on something other than expert information. Proposing a nonparametric method that uses B-splines for approximation, Chen et al. (2014) claims that nonparametric techniques are asymptotically robust if the demand function is sufficiently smooth. The authors also show that misspecified parametric methods can cause substantial revenue losses.

Here, we propose differentiating models based on their demand function as seen in den Boer (2015). The demand function may be static or dynamic. Unlike static demand functions, where changes in pricing are motivated by limited capacity, we model demand via uni- and bivariate functions of price and other covariates. This setting renders the demand function dynamics for confounding variables such as time. We contribute to nonparametric dynamic pricing by non-linear relationships of demand and price to confounding variables, which can also influence price sensitivity. We achieve this goal via a bivariate and penalized B-spline setting. The resulting dynamic pricing algorithm relies on price derivatives, which change dynamically over confounding variables. To consider scarce capacity, we assume known opportunity cost to evaluate the margin and cost component separately. This assumption enables subsequent optimization steps to consider separate capacity allocation and revenue maximization. Revenue maximization solves a Cournot-type price optimization problem. Pölt et al. (2018) describes a similar concept, concentrating on capacity allocation.

Our work also contributes to research on price endogeneity. Price endogeneity causes biased sensitivity estimates: Mumbower et al. (2014), Lo et al. (2015), and Petrin and Train (2010) show that ignoring price endogeneity means underestimating the price coefficient. Typically, instrument variables are suggested to cure endogeneity. Usually, the instrument variable is a linear combination of (presumably) exogenous variables. Given a fitting instrument variable, unbiased estimates result from a two-staged estimation procedure (Davidson and MacKinnon 1999).

In recent times, driven by the COVID-19 pandemic, the surge in inflation since mid-2021, and the start of the Ukraine war in April 2022, the models' capability to adjust to changing market conditions has become an important feature. As described by Yeoman (2021), airlines need to accept COVID-19 as the new norm until the coronavirus pandemic disappears from this planet. Yeoman (2022), analyses the impact of the Ukraine war and inflation on price sensitivity and demand. To adjust how revenue management is performed, Vinod (2021) suggests monitoring key revenue management metrics and taking corrective action with demand and supply levers to make the revenue plan happen. To perform corrective actions using the presented model framework of this paper, Bonciolini (2022) presented a price elasticity monitoring method that automatically adjusts price elasticity estimates. Similarly to adjustments to price elasticity, Pinheiro et al. (2022) introduced a shock detector to identify positive and negative shocks in demand volume and willingness-to-pay. Besides applying adjustments as proposed by Bonciolini (2022), our work shows that the changing market conditions caused by the COVID-19 pandemic can be considered by adding additional functions to the model.

Statistical model and estimation

This section outlines the statistical model class and introduces parameter estimation based on a penalised likelihood procedure (e.g. Eilers and Marx 1996). The proposed approach considers multivariate functional dependencies between price and additional covariates to capture the unknown structure of price sensitivity. However, it does not assume a known functional form but approximates functional components via penalised splines. A penalised spline approximates an unknown function by a linear combination of basis functions. Common bases are B-splines (de Boor 1978), cubic (Gu 2002, p. 2) or, thin-plate splines (Wood 2017, p. 150). We refer to Wood (2017) for technical details and to Marx et al. (2016) for a general overview.

To improve the validity of price-sensitivity estimates (Tutz and Leitenstorfer 2007) and to disentangle changes in the volume of demand and related pricing effects, the proposed method combines the penalised smoothing spline ANOVA type interaction model of Lee and Durbán (2011) with the shape-constrained generalised additive model framework of Pya and Wood (2014). Similar to Blundell et al. (2012) or Brezger and Steiner (2008), a monotonicity constraint on functions that contain price is imposed, ensuring that demand decreases when price increases.

Model development

Let index $i = 1, \ldots, M$ describe a flight connection between two cities, where M represents the total number of flights to be analysed. Let $N_i(t)$ define the number of accumulated bookings for flight i at the time $t \in \left[t_i^{\text{open}}, t_i^{\text{close}}\right]$, where the interval represents the sales horizon during which flight i is offered. Indexing t_i^{open} and t_i^{close} of the sales horizon by i allows for individual sales horizons per flight. We assume that $N_i(t_i^{\text{open}}) \equiv 0$, i.e., there are no observed bookings at the beginning of the sales horizon.

We model the accumulated bookings $N_i(t)$ as a Poisson process, such that the increments, $N_i(t) - N_i(t-1)$ are Poisson-distributed with

$$P\Big(\big\{N_i(t) - N_i(t-1)\big\} = y_{i,t}\Big) = \frac{\lambda(t)^{y_{i,t}}}{y_{i,t}!}\exp\big(-\lambda(t)\big). \tag{1}$$

Eq. (1), also includes the possibility of observing no bookings ($y_{i,t} = 0$, referred to as non-bookings). The Poisson intensity $\lambda(t)$ accounts for changes in booking intensity and depends on price and additional observable covariates. The covariates for flight i at time t with price $p_{i,t}$ are given by a covariate vector $\mathbf{x}_{i,t} = \big(x_{1,i,t}, \ldots, x_{K_2,i,t}, p_{i,t}, z_{1,i,t}, \ldots, z_{K_1,i,t}\big)$. The index-sets $I_1 = \{1, \ldots, K_1\}$ and $I_2 = \{1, \ldots, K_2\}$ give the positions of the categorical covariates $x_{k,i,t}, (k \in I_1)$ and continuous covariates $z_{k,i,t}, (k \in I_2)$. For categorical covariates in I_1, the k^{th} variable takes values from the set $J_k = \{1, \ldots, G_k\}$. This leads to the model:

$$\lambda(\mathbf{x}_{i,t}, t) = \lambda\big(x_{1,i,t}, \ldots, x_{K_2,i,t}, p_{i,t}, z_{1,i,t}, \ldots, z_{K_1,i,t}, t\big). \tag{2}$$

The model aims to quantify the effect of price on booking intensity given covariates $z_{k,i,t}, (k \in I_2)$ and $x_{k,i,t}, (k \in I_1)$. Thus, the effects of covariates on booking intensity need to be specified. To this end, the model captures all bivariate interaction effects of the continuous covariates by setting

$$\begin{aligned}
&\log\Big(\lambda(\mathbf{x}_{i,t}, t)\Big) \\
&\quad = \beta_0 + \sum_{k \in I_1}\sum_{j \in J_k} \mathbf{1}_{\{x_{k,i,t}=j\}}\beta_{k,j} \\
&\qquad + f_p\big(p_{i,t}\big) + f_{p,t}\big(p_{i,t}, t\big) + \sum_{k \in I_2} f_{p,k}\big(p_{i,t}, z_{k,i,t}\big) \\
&\qquad + f_t(t) + \sum_{k \in I_2} f_k\big(z_{k,i,t}\big) + \sum_{k \in I_2} f_{t,k}\big(t, z_{k,i,t}\big) \\
&\qquad + \sum_{\substack{k_1 < k_2 \\ k_1, k_2 \in I_2}} f_{k_1,k_2}\big(z_{k_1,i,t}, z_{k_2,i,t}\big).
\end{aligned} \tag{3}$$

Here, $\mathbf{1}_{\{x_{k,I,t}=j\}}$ is an indicator function that equals one if the categorical covariate $x_{k,i,t} = j \in J_k$. The coefficient-vector $\boldsymbol{\beta}_{k \in I_1} = (\beta_{k,1}, \ldots, \beta_{k,G_k})$ quantifies the effect of the k^{th} categorical variable on the booking intensity. Similar to a full factorial design, which analyses the effect of each covariate as represented by the univariate function $f(\cdot)$, bivariate function $f(\cdot,\cdot)$ captures all interactions between covariates. For example, $f_p\big(p_{i,t}\big)$ determines the general level of price-sensitivity, and $f_t(t)$ describes the dynamics in the arrival of bookings. The interaction effect $f_{p,t}\big(p_{i,t}, t\big)$ quantifies how price sensitivity changes over the sales horizon.

To describe price sensitivity, we first isolate demand components unrelated to price. These are captured by price-independent functions $f_t(\cdot), f_{k \in I_2}(\cdot)$, and $f_{t,k \in I_2}(\cdot,\cdot), f_{\substack{k_1 < k_2 \\ k_1, k_2 \in I_2}}(\cdot,\cdot)$. In contrast, $f_p(\cdot), f_{p,t}(\cdot,\cdot)$, and $f_{p,k \in I_2}(\cdot,\cdot)$ amend the slope of price, representing price-sensitivity. When demand is price-sensitive, fewer bookings occur if the price is high, and more bookings occur if the price is low. Monotonicity constraints as proposed in Pya and Wood (2014) for functions $f_p(\cdot), f_{p,t}(\cdot,\cdot)$, and $f_{p,k \in I_2}(\cdot,\cdot)$ ensure this. Appendix 1 provides a detailed description and a technical discussion of the penalty setup. Furthermore, Appendix 2 outlines the implementation to consider price endogeneity during the estimation process.

Empirical data

To demonstrate the proposed approach, we apply it to airline booking data.

The empirical data set includes 1, 708, 236 bookings ($y_{i,t} > 0$) for the economy compartment as offered on eight European city pairs between April 1, 2012, and December 31, 2015. Eight pairs of origin and destination (OD) create 16 point-to-point (P2P) connections, as passengers can travel each connection in two directions. Each flight i is described by the continuous covariates departure day of the year (YDAY, taking values from $1, \ldots, 365$) and departure time (DTIME, taking values between 0 and 24). The dataset also includes daily snapshots of the lowest available fare ($p_{i,t}$). Each booking is attributed to one of 16 P2P connections and one of the 10 to 14 fares offered.

When the airline records no bookings for flight i on the day t, a non-booking entry ($y_{i,t} = 0$) reports the offered price. Entries are further described by the categorical covariates booking weekday (BDAY, taking the values Monday, …, Sunday), the departure weekday (DDAY, taking the values Monday, …, Sunday), and the P2P connection. Flight, booking, and availability data create a complete record of available and booked fares for the entire booking horizon. The daily snapshot only covers price

changes within one booking day. Therefore, when multiple bookings for different prices occur on the same day, $p_{i,t}$ is observed at a finer resolution than per day t. Appendix 3 describes how an extension of model (3) compensates for this.

We exclude flight departures on public or school holidays, major fairs, exhibitions, or conferences. If a flight is cancelled or re-scheduled, we maintain data from before the adjustment and treat data collected after the change as a new flight. In consequence, we consider 70,283 flights and 3,225 departure days.

Our analysis excludes bookings of fares with fewer restrictions than the lowest available fare. From a pricing point of view, the revenue gain from such upselling could be modelled separately. Here, we aim only to find the best price for the basic fare, as ancillary features could complicate the estimation of the price sensitivity.

The analysis only considers ticketed bookings. It focuses on return tickets, which represent 95.5% of all bookings. Finally, to reduce the number of non-bookings, it only considers the slice of the sales horizon that captures 99% of bookings. Table 1 summarises the analysed data set.

The first row lists the number of days in the sales horizon considered. The second row describes the number of daily services. Row three and four report the number of bookings ($y_{i,t} > 0$) and non-bookings ($y_{i,t} = 0$).

The airline's pricing model

As discussed in Appendix 2, a prediction model for the airline's pricing and a suitable instrument variable are required to account for price endogeneity. As airline revenue management assumes fixed and variable costs to be constant across flights operating on the same route, these cost types are unsuitable instruments. Instead, we propose to use the opportunity cost of capacity as an instrument variable.

Airline revenue management often employs the opportunity cost of capacity as a bidprice for capacity allocation. The bidprice is known for future departure days and varies across bookings, as each booking increases the bidprice to acknowledge scarce capacity. This mechanism introduces simultaneity between demand and price, i.e., price influences demand and vice versa. Furthermore, when flights are part of a transfer itinerary, the bidprice accounts for network effects. Therefore, the bidprice is not entirely determined by the demand for a single flight.

However, this instrument variable only varies if the capacity is scarce. Therefore, it is only useful when demand exceeds capacity. When the natural logarithm of the bidprice is the instrument $\mathrm{IV}_{i,t}$, the functional structure of the first-stage regression equation (16) is:

$$\eta_{i,t} = \theta_0 + \theta_1 \log(\mathrm{IV}_{i,t}) + \sum_{j=1}^{6} \mathbf{1}_{\mathrm{BDAY}_{i,t}=j}\theta_{1,j} + s_t(t) + s_1(\mathrm{DTIME}_{i,t}) + s_2(\mathrm{YDAY}_{i,t}). \tag{4}$$

Table 1 Summary of data for the origin–destination pairs OD1 to OD8

Origin destination pair	Booking horizon	Daily services	Bookings	Non-bookings
OD1	291	6	101,905	1,193,193
OD2	285	8	192,764	2,007,423
OD3	254	12	280,130	3,339,491
OD4	208	4	36,076	887,384
OD5	282	5	99,077	1,339,820
OD6	110	15	406,884	621,838
OD7	110	16	320,067	448,388
OD8	106	17	271,333	425,446

The airline's demand model

The empirical data set records three categorical covariates: DDAY, BDAY, and P2P. Segmenting by the DDAY and P2P induces a full interaction between these variables and any other covariate that describes the demand model (2). Therefore, we estimate $7 \times 16 = 112$ separate models at this level. As the categorical variable BDAY is closely associated with the booking time t, the model includes it to capture potential changes in booking intensity over the sales horizon. Including BDAY as the only categorical variable (taking BDAY=Sunday as the reference category) yields the first index set as $I_1 = \{1\}$ with $J_1 = \{1, \ldots, 6\}$, where 1 represents Monday, 2, Tuesday,...,6 Saturday.

In addition to price $p_{i,t}$ and booking time t, the data records continuous covariates DTIME and YDAY. $I_2 = \{1, 2\}$ defines the second index set. The covariate vector is, therefore $\mathbf{x}_{i,t} = (\mathrm{BDAY}_{i,t}, p_{i,t}, \mathrm{DTIME}_{i,t}, \mathrm{YDAY}_{i,t}, t)$. Thus, a typical data row for flight i with booking day Monday (reported as 1), ticket price \$50, departure time 6:00 am (reported as 6), and departure date on January 2 (reported as 2) at the day of departure ($t = 0$) is $\mathbf{x}_{i,t} = (1, 50, 6, 2, 0)$. The airline's demand model is as follows:

$$\begin{aligned}\log\left(\lambda(\mathbf{x}_{i,t}, t)\right) = {} & \beta_0 + \beta_{\widehat{\xi}}\widehat{\xi}_{i,t} + \sum\nolimits_{j=1}^{6} \mathbf{1}_{\mathrm{BDAY}_{i,t}=j}\beta_{1,j} + f_p(p_{i,t}) \\ & + f_{p,t}(p_{i,t}, t) + f_{p,1}(p_{i,t}, \mathrm{DTIME}_{i,t}) \\ & + f_{p,2}(p_{i,t}, \mathrm{YDAY}_{i,t}) \\ & + f_t(t) + f_1(\mathrm{DTIME}_{i,t}) + f_2(\mathrm{YDAY}_{i,t}) \\ & + f_{t,1}(t, \mathrm{DTIME}_{i,t}) + f_{t,2}(t, \mathrm{YDAY}_{i,t}) \\ & + f_{1,2}(\mathrm{DTIME}_{i,t}, \mathrm{YDAY}_{i,t}).\end{aligned} \tag{5}$$

Here, coefficient-vector $\boldsymbol{\beta}_1 = (\beta_{1,1}, \ldots, \beta_{1,6})$ quantifies the effect of the booking day on the demand intensity.

Estimation results

We look at one route, OD8, and DDAY = Thursday, to demonstrate the estimation results. Figure 1 shows the smooth components $s_t(t), s_1(\text{DTIME}_{i,t})$, and $s_2(\text{YDAY}_{i,t})$ from the first-stage. The left panel shows the estimate of $s_t(t)$, which indicates that prices increase over the sales horizon. The estimate of $s_1(\text{DTIME})$ (middle panel) shows there exists a strong departure time pattern. Flights departing around 8:00 am and 7:00 pm are the most expensive. The right panel shows the estimate of $s_2(\text{YDAY})$. The lack of a strong pattern indicates little price variation over the days of the year.

Figure 2 shows second-stage estimates of demand model (5).

Our analysis concentrates on four aspects. All covariates except the one indicated in the caption are fixed in each panel. The panels on the left reveal how price and demand vary over departure time (a) and year day (c). Panels (b) and (d) show how demand varies independently of the price. Panel (a) indicates that price sensitivity depends on departure time. Peak flights at 7:00 am and 7:00 pm show a smaller price slope than midday flights. Panel (c) accounts for seasonal price sensitivity changes but only shows moderate fluctuations. Panel (b) confirms that demand varies along the time-to-departure axis by departure time. The step-like pattern in panel (b) arises from the influence of BDAY: fewer bookings occur on weekends than on weekdays.

Table 2 reports the parameter estimates of the first (4) and second-stage (5), as well as the estimated standard errors (in brackets).

The parameter estimates for the second stage show fewer bookings on weekends than on weekdays. When the second stage considers price endogeneity, there are about ten times more bookings for BDAY=Monday than on the reference category BDAY=Sunday ($\exp(-2.01) \approx 0.13$ to $\exp(-2.01 + 2.29) \approx 1.32$). For the first stage, BDAY estimates are negative for weekdays and positive for the weekend. Thus, weekdays combine high demand with low prices, while weekends combine low demand with high prices. Apart from the BDAY effect, we also report the estimates of IV (only relevant for the first stage) and first-stage residual $\widehat{\xi}$ (only suitable for the second stage). In the first stage, IV is significantly different from zero (with t-statistic $= 0.07/0.0004 = 175$), which satisfies one requirement of the two-staged procedure. The parameter estimate for the first-stage residual $\widehat{\xi}$ represents the working parameter of a univariate spline with one inner knot-interval and a monotonicity restriction according to Pya (2010 p. 45). The BDAY estimates show that considering the first-stage residual $\widehat{\xi}$ does not change the parametric coefficients of BDAY. As the second stage, which controls for price endogeneity, shows smaller values for AIC and

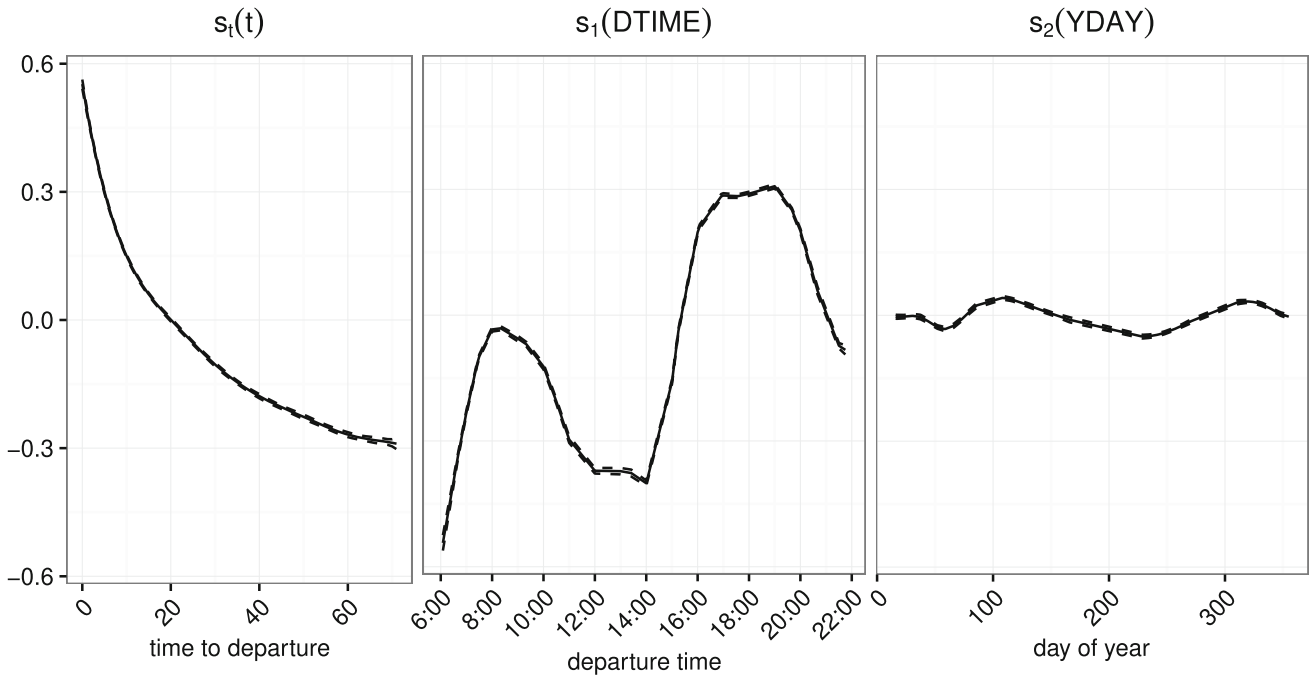

Fig. 1 Estimate of the three smooth functions $s_t(t), s_1(\text{DTIME})$, and $s_2(\text{YDAY})$ for the first-stage model (4). Solid line = estimate, dotted lines = 99% confidence band

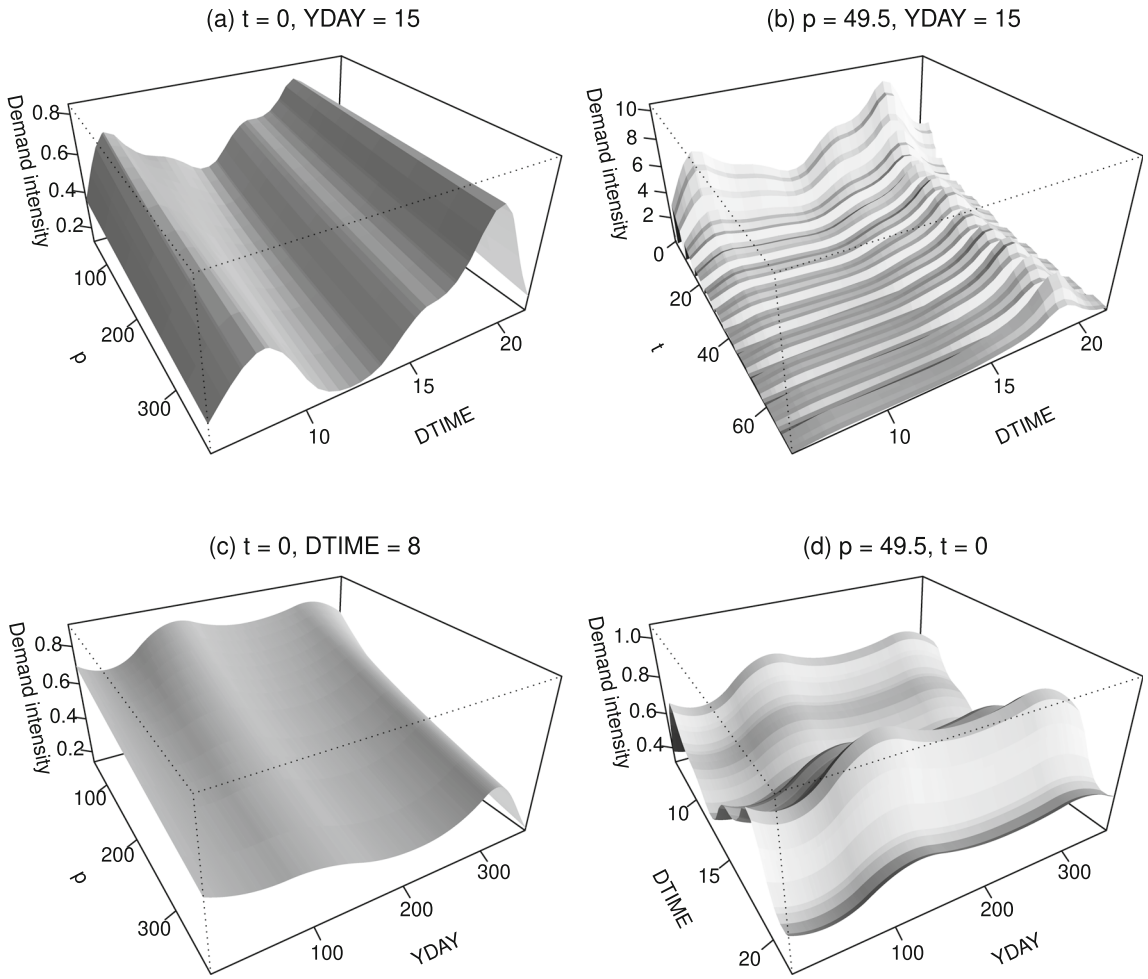

Fig. 2 Estimates of the conditional demand intensity for OD8 and DDAY = Thursday. The variables appearing in each panel's title are fixed to a specific value (e.g., t is fixed to 0 and YDAY to 15 for panel (**a**). Every panel shows how the demand intensity (vertical axis) changes within the covariates that are shown at the horizontal axis (e.g., the demand intensity within the panel (**a**) changes in departure time and peaks at 8:00 am and 7.00 pm)

BIC, the remainder of the paper focuses on the corresponding model setup with endogeneity considered. In Appendix 4, the models' prediction accuracy assessment is discussed.

Dynamic pricing

This section demonstrates the demand model's applicability to dynamic pricing. The resulting pricing leads to an offered price that maximises the revenue gained from sales.

Continuous prices

This paper assumes dynamic pricing with support on $\mathbb{R}_+$ is possible. With revenue gain $r_{i,t}$ from selling a ticket at a price $p_{i,t}$, we calculate the total revenue as $\lambda(\mathbf{x}_{i,t}, t)r_{i,t}$. The opportunity cost of selling capacity to $\lambda(\mathbf{x}_{i,t}, t)$ many passengers is $\lambda(\mathbf{x}_{i,t}, t)\pi_{i,t}$. When the capacity constraint is irrelevant, we can set $\pi_{i,t} = 0 \; \forall \; i, t$. According to Eq. (2), the proposed demand model includes a multiplicatively separable demand rate with exponential price sensitivity. From this, we derive the optimal price $p^{\star}_{i,t}$ by solving

$$\begin{aligned} &\max_{p_{i,t}} \left\{ \lambda(\mathbf{x}_{i,t}, t)r_{i,t} - \lambda(\mathbf{x}_{i,t}, t)\pi_{i,t} \right\} \\ &\Leftrightarrow \frac{\partial\left(\lambda(\mathbf{x}_{i,t}, t)r_{i,t} - \lambda(\mathbf{x}_{i,t}, t)\pi_{i,t}\right)}{\partial p_{i,t}} \stackrel{!}{=} 0. \end{aligned} \tag{6}$$

To efficiently calculate the derivative of $\lambda(\mathbf{x}_{i,t}, t)$ concerning $p_{i,t}$, we can take advantage of the fact that the derivative of a B-spline is a linear combination of lower order B-splines (Marsh and Marshall 1999). Solving (6), i.e., maximising the total revenue gain over cost, yields the optimal value for $r_{i,t}$, say $r^{\star}_{i,t}$. To calculate the corresponding optimal price-value $p^{\star}_{i,t}$, we have to derive the

Table 2 Parameter estimates for OD8 and DDAY = Thursday

	Stage		
	First	Second	
		Endogeneity considered	
		Yes	No
Intercept	4.8223(0.0022)	−2.0104(0.3877)	−1.8381(0.1084)
log(IV)	0.0700(0.0004)	–	–
$\widehat{\xi}$	–	−0.0020(0.0013)	–
BDAY = Monday	−0.0253(0.0025)	2.2966(0.1123)	2.2946(0.0358)
BDAY = Tuesday	−0.0293(0.0025)	2.2116(0.1311)	2.2079(0.0452)
BDAY = Wednesday	−0.0263(0.0025)	2.2363(0.1406)	2.2326(0.0498)
BDAY = Thursday	−0.0224(0.0025)	2.1077(0.1366)	2.1019(0.0504)
BDAY = Friday	−0.0129(0.0025)	2.1083(0.1273)	2.1050(0.0460)
BDAY = Saturday	0.0064(0.0028)	−0.3627(0.1692)	−0.3627(0.0516)
AIC	1457362	106957.9	107131.0
BIC	4741586	107920.4	108034.5

Standard errors in brackets

amount of variable cost (including fuel, onboard service, and taxes) that has to be added to $r_{i,t}$ to achieve price $p_{i,t}$ (the amount is defined by the difference $p_{i,t} - r_{i,t}$). We do so by solving the regression problem

$$\begin{aligned} p_{i,t} - r_{i,t} &= \alpha_0 + \alpha_1 p_{i,t} + \epsilon_{i,t} \\ r_{i,t} &= \underbrace{-\alpha_0}_{\equiv\gamma_0} - \underbrace{(1-\alpha_1)}_{\equiv\gamma_1} p_{i,t} + \epsilon_{i,t}. \end{aligned} \tag{7}$$

The difference between $r^{\star}_{i,t}$ and $p^{\star}_{i,t}$ is determined by $\gamma_0 = -\alpha_0$ and $\gamma_1 = 1 - \alpha_1$. The parameter α_0 represents the constant variable cost amount that does not depend on the ticket price, e.g., fuel or onboard service. The parameter α_1 gives the variable cost factor that increases the price, e.g., taxes. If model (3) is linear in $p_{i,t}$, the maximization problem (6) has the closed-form solution

$$p^{\star}_{i,t} = \underbrace{-\frac{1}{\mathbf{1}_{2\mathrm{s}}\beta_{\widehat{\xi}} + f'_p + f'_{p,t}(t) + \sum_{k\in I_2} f'_{p,k}(z_{k,i,t})}}_{\text{profit margin}} + \underbrace{\frac{\alpha_0}{1-\alpha_1} + \frac{\pi_{i,t}}{1-\alpha_1}}_{\text{cost margin}}. \tag{8}$$

A detailed description of how to derive (8) by solving (6) is found in Appendix 6. Here, $f'_p, f'_{p,t}(t)$, and $f'_{p,k}(z_{k,i,t})$ correspond to the derivative of $f_p, f_{p,t}(t), f_{p,k}(z_{k,i,t}), k \in I_2$ with respect to $p_{i,t}$, e.g., $f'_p = \frac{\partial f_p(p_{i,t})}{\partial p_{i,t}}$. Assuming linearity of $p_{i,t}, f'_p$ is only a scalar. Factor $\beta_{\widehat{\xi}}$ only appears in (8) if $\mathbf{1}_{2\mathrm{s}}$ indicates that price endogeneity is considered, where $\mathbf{1}_{2\mathrm{s}} = 1$ if the estimation is two-staged and $\mathbf{1}_{2\mathrm{s}} = 0$ otherwise. The influence of $\widehat{\xi}$ is constrained such that $\beta_{\widehat{\xi}} < 0$.

By monotonicity of (2) within $p_{i,t}$, every derivative $f'_p, f'_{p,t}(t), f'_{p,k}(z_{k,i,t})$ is strictly negative, rendering the profit margin positive. The smooth components $f_t, f_k, f_{t,k}, f_{k_1,k_2}$, $k, k_1, k_2 \in I_2, k_1 < k_2$ and parametric parts $x_{k,i,t}, (k \in I_2)$ are not relevant to price-sensitivity and vanish when the derivative of $p_{i,t}$ is calculated. Thus

$$\frac{\partial \lambda(\mathbf{x}_{i,t}, t)}{\partial p_{i,t}} = \lambda'(\mathbf{x}_{i,t}, t) = \mathbf{1}_{2\mathrm{s}}\beta_{\widehat{\xi}} + f'_p + f'_{p,t}(t) + \sum_{k\in I_2} f'_{p,k}(z_{k,i,t}) < 0$$

.

Figure 3 shows how each OD's derivative $\lambda'(\mathbf{x}_{i,t}, t)$ evolves over DTIME for DDAY=Thursday, $t = 0$, and YDAY=15. Note that decreasing price-sensitivity goes along with increasing $\lambda'(\mathbf{x}_{i,t}, t)$. Aside from the amplitude of the pattern, every OD experiences a decline in price-sensitivity during the morning and evening ($|\lambda'(\mathbf{x}_{i,t}, t)|$ becomes smaller), meaning that passengers are willing to pay more if travelling during these hours of the day.

As (8) shows, $p^{\star}_{i,t}$ is the sum of the profit margin and cost. Whenever price-sensitivity decreases, the value of $\lambda'(\mathbf{x}_{i,t}, t)$ increases. Therefore, the optimal price $p^{\star}_{i,t}$ increases by the increasing value of the profit margin. Thus, the offered price $p^{\star}_{i,t}$ inversely depends on the estimated price sensitivity. The lower bound of $p^{\star}_{i,t}$ is the cost of production. Depending on the application, this bound is also a function of opportunity cost $\pi_{i,t}$.

Figure 4 shows $p^{\star}_{i,t}$ for $t = 0$, DDAY=Thursday, and day of the year 15 for OD6 and OD8 with opportunity cost $\pi_{i,t} \in \{1, 20, 100\}$. Appendix 7 induces supplementary illustrations for the other OD.

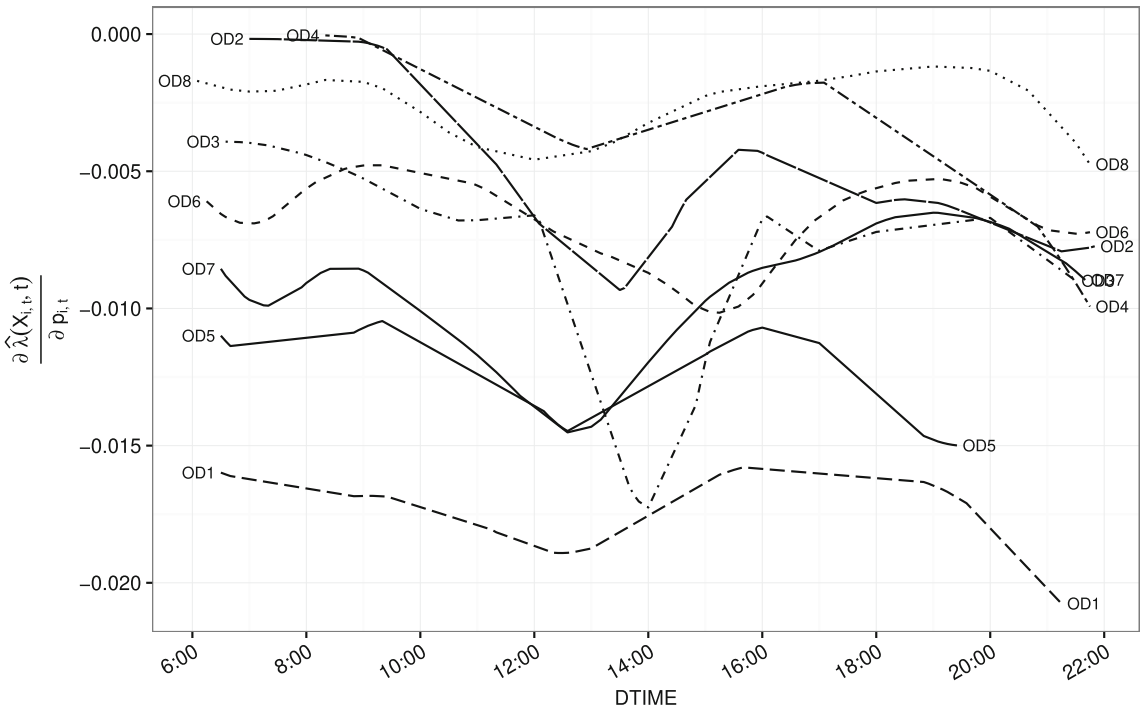

Fig. 3 Estimated derivative $\widehat{\lambda}'(\mathbf{x}_{i,t}, t)$ for DDAY=Thursday, t=0 and YDAY=15 for different DTIME values. Each line shows the changes of the derivative $\widehat{\lambda}'(\mathbf{x}_{i,t}, t)$ for a specific OD

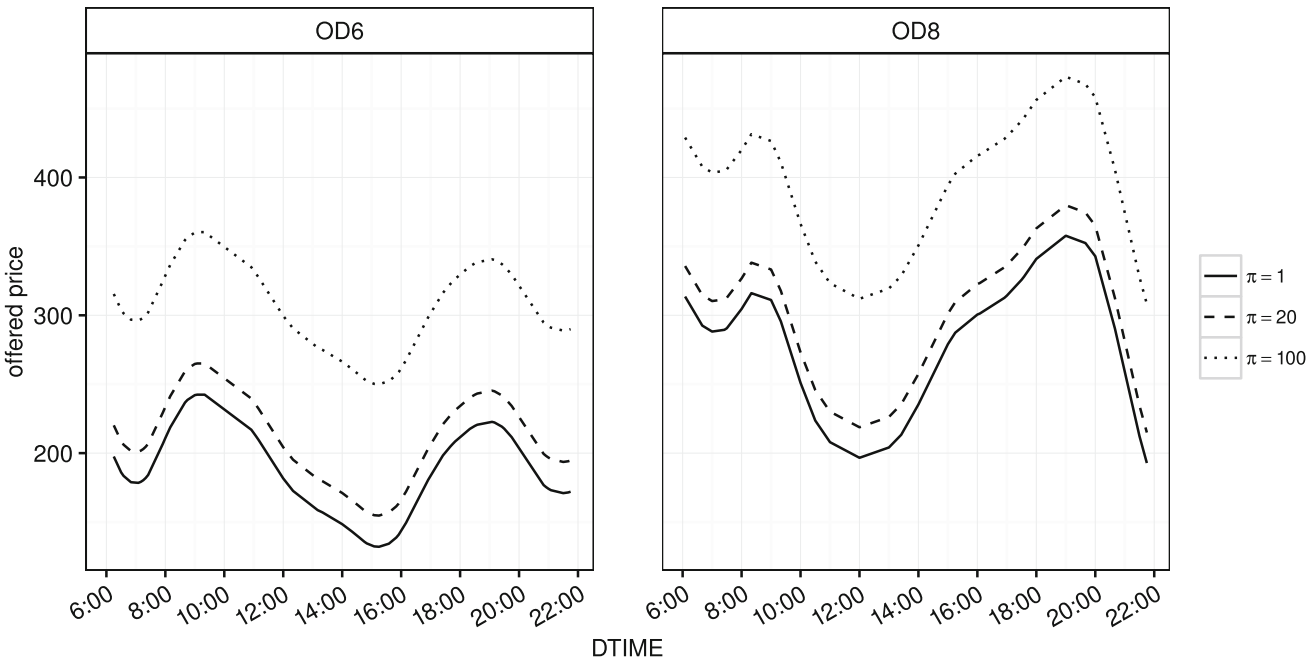

Fig. 4 Optimal price values for OD6, OD8 at DDAY=Thursday for opportunity cost $\pi_{i,t} = 1, 20, 100$

The general shape of each curve is defined by the derivative function $\lambda'(\mathbf{x}_{i,t}, t)$ as shown by Fig. 3. For OD6, optimal price $p^{\star}_{i,t}$ increases if the value of the derivative function $\lambda'(\mathbf{x}_{i,t}, t)$ increases, indicating a decrease in price-sensitivity. This mechanic leads to a pricing policy where prices inversely depend on price sensitivity, i.e., the price increases if the price sensitivity decreases and vice versa. For OD8, this yields higher prices for peak flights, as an increase within the derivative function $\lambda'(\mathbf{x}_{i,t}, t)$ indicates a decrease in price sensitivity. Additionally, a change in the

Table 3 Layout of the test pattern

	OD1,OD2, and OD4							OD3						
	Outbound direction													
CW	Mo	Tu	We	Th	Fr	Sa	Su	Mo	Tu	We	Th	Fr	Sa	Su
25	o	x	o	x	o	x	o	x	o	x	o	x	o	x
24	x	o	x	o	x	o	x	o	x	o	x	o	x	o
23	o	x	o	x	o	x	o	x	o	x	o	x	o	x
22	x	o	x	o	x	o	x	o	x	o	x	o	x	o
	Inbound direction													
25	x	o	x	o	x	o	x	o	x	o	x	o	x	o
24	o	x	o	x	o	x	o	x	o	x	o	x	o	x
23	x	o	x	o	x	o	x	o	x	o	x	o	x	o
22	o	x	o	x	o	x	o	x	o	x	o	x	o	x

Abbreviations: x = influenced, o = non-influenced

opportunity cost π shifts the entire curve as the cost of selling a seat increases, regardless of price sensitivity.

Discrete prices

For most airlines, technological hurdles still call for offering prices from a countable and finite set of discrete values $\Omega_p = \{p_1, \ldots, p_J\}$ with revenue gain $r_j,\ j \in \{1, \ldots, J\}$ (compare Fiig et al. 2015). As suggested by Fiig et al. (2010), we also propose only to offer the subset of prices $\Omega'_p \subset \Omega_p$ for which the marginal revenue gain exceeds the marginal cost (bid-price). As it turns out (proof given in Appendix 5), the solution of the continuous problem (8) also defines the boundary point for price points that belong to the set Ω'_p. Therefore, it is optimal to offer the next highest price point to the optimal price $p^{\star}_{i,t}$.

Performance evaluation in a field study

In cooperation with a European network airline, we test our model in a field study. To that end, we choose four OD to reflect specific market characteristics, e.g., the dominance of business vs. leisure travellers or high versus low competition. OD1 and OD4 represent leisure routes, whereas OD2 and OD3 represent business routes. Applying our approach to every combination of OD, DDAY, and P2P created $4 \times 7 \times 2 = 56$ separate model estimates. For every model, we offer (given the bidprice) the next highest price, the optimal price $p^{\star}_{i,t}$.

The field study includes departure dates from 2016-05-30 until 2016-06-26. For every flight within that departure period and booking dates between 2016-04-04 and 2016-05-29, the available price is chosen according to the optimal price $p^{\star}_{i,t}$ (see 5.2). Table 3 describes the test pattern.

Table 4 Results of the live test in percent

Market	OD1	OD2	OD3	OD4	overall
Revenue	1.64%	6.31%	8.44%	8.03%	6.37%
Margin	36.39%	18.96%	13.91%	11.08%	15.36%

The checkerboard pattern aims to capture and control systematic differences in DDAY and OD directions. The airline's regular revenue management system (non-influenced) calculates the bidprices and lets market analysts set the prices. Both the traditional approach and our model relied on the same bidprice information. Thus, the observed revenue difference originates from the passengers' price sensitivity estimates. The overall revenue gain is aggregated separately for influenced and non-influenced departure days for each OD. The difference is given in percent of the regular system's performance. As the results in Table 4 show, our approach successfully increased the revenue between 1.64% to 8.03% and the margin by 11.08% to 36.39% across markets. The margin defines the gaps between revenue earned and opportunity cost π. Due to the positive outcome, the airline plans to apply our approach to every OD of the European network by the end of 2017.

Model adjustments due to market turbulences

Since 2017 and due to the success of the field study, see "Performance evaluation in a field study" section, AirABC decided to increase the models' scope to about 360 ODs. In May 2019, an intervention analysis examining the revenue impact of the models' rollout resulted in an average

revenue increase of +2.37%, confirming the field study's positive result. Since the models' rollout, the price elasticity estimates are regularly updated using the past two departure years. Even though frequent updates of the demand model would eventually catch up with a changing market environment, due to the functional structure of the predictor (5), the price-elasticity estimates for the next selling date only differ from the previous selling date by variables that describe the flight (DTIME, YDAY) and the time to departure t. Specifically, structural changes within the market happening from one selling date to another cannot be captured accurately. To allow for more flexibility for demand- and price-elasticity predictions to describe changes in the market environment, four additional covariates are introduced:

1. Booking day of the year (BYDAY), taking values from $1, \ldots, 365$
2. Selling Date Index (SDI) as
   (a) SDI = -630 for April 12, 2019
   (b) ...
   (c) SDI = -2 for December 30, 2019
   (d) SDI = -1 for December 31, 2019
   (e) SDI = 0 (ease of interpretation) for the selling date January 1, 2020
   (f) SDI = 1 for January 2, 2020
   (g) SDI = 2 for January 3, 2020
   (h) ...
   (i) SDI = 100 for April 11, 2021
3. Daily new cases of COVID-19 within the country of the origin airport (OCOV)
4. Daily new cases of COVID-19 within the country of the destination airport (DCOV)

The data for daily new cases of COVID-19 is gathered from OWID (2021). Figure 5 shows how the daily new cases of COVID-19 evolved over the period 2020-01-24 to 2021-04-11. For every country, the first wave of COVID-19 cases occurred from 2020-03-01 to 2020-05-01 and was followed by another wave starting between 2020-08-01 and 2020-10-01. Within 2021-05-01 and 2021-08-01, the number of cases was reduced by severe lock-down measures, which were (depending on the country) partially lifted during the summer months, i.e., between 2020-06-01

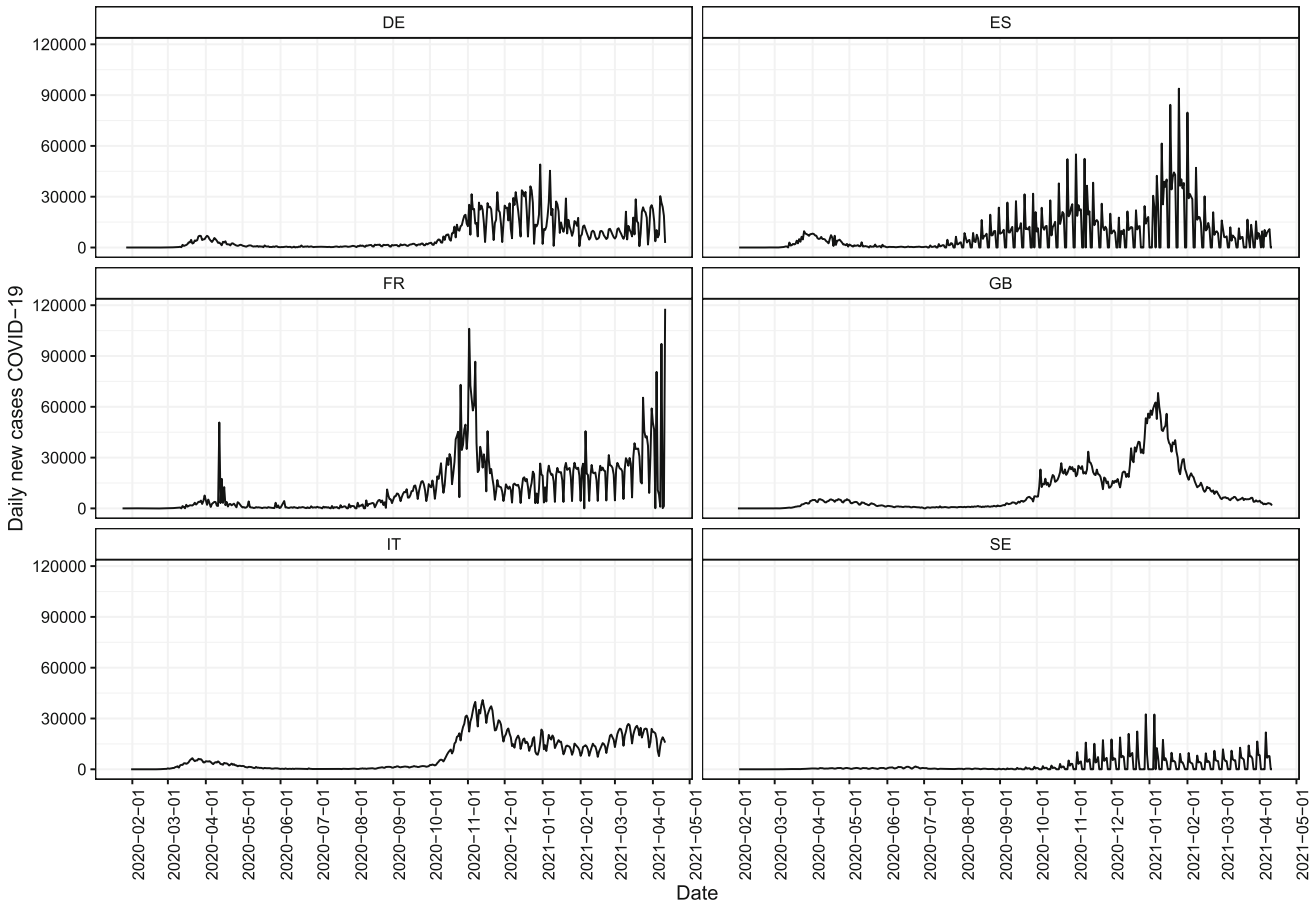

Fig. 5 Daily new cases of COVID-19 for the countries Germany(DE), Spain (ES), France (ES), United Kingdom (GB), Italy (IT), and Sweden (SE) from 2020-01-24 to 2021-04-11

Table 5 Additional model functions and covariates allowing for more flexibility for demand- and price-elasticity predictions

Function	Description
$f_{p,3}(p_{i,t},\ \text{BYDAY}_{i,t})$	Booking yearday seasonality of price elastictiy
$f_3(\ \text{BYDAY}_{i,t})$	Booking yearday seasonality of demand
$f_{p,4}(p_{i,t},\ \text{SDI}_{i,t})$	Daily change in price elasticity
$f_4(\ \text{SDI}_{i,t})$	Daily demand changes
$f_{p,5}(p_{i,t},\ \text{OCOV}_{i,t})$	Change of price elasticity by daily new COVID19 cases at the origin airport
$f_5(\ \text{OCOV}_{i,t})$	Demand changes by daily new COVID19 cases at the origin airport
$f_{p,6}(p_{i,t},\ \text{DCOV}_{i,t})$	Change of price elasticity by daily new COVID19 cases at the destination airport
$f_6(\ \text{DCOV}_{i,t})$	Demand changes by daily new COVID19 cases at the destination airport
$f_{t,5}(t,\ \text{SDI}_{i,t})$	Daily change of the demand booking curve

to 2020-08-01 and re-implemented afterward. The adjustment of model (5), including the additional covariates (in black), is defined by Eq. (9). Table 5 describes the nine functions in more detail.

$$\begin{aligned}\log\left(\lambda(\mathbf{x}_{i,t},t)\right)^{\text{adj}} = \log\left(\lambda(\mathbf{x}_{i,t},t)\right)\\ +f_3(\ \text{BYDAY}_{i,t}) + f_4(\ \text{SDI}_{i,t})\\ +f_5(\ \text{OCOV}_{i,t}) + f_6(\ \text{DCOV}_{i,t})\\ +f_{p,3}(p_{i,t},\ \text{BYDAY}_{i,t}) + f_{p,4}(p_{i,t},\ \text{SDI}_{i,t})\\ +f_{p,5}(p_{i,t},\ \text{OCOV}_{i,t})\\ +f_{p,6}(p_{i,t},\ \text{DCOV}_{i,t})\\ +f_{t,5}(t,\ \text{SDI}_{i,t}).\end{aligned} \tag{9}$$

where $\log\left(\lambda(\mathbf{x}_{i,t},t)\right)$ corresponds to the (unadjusted) model (3). Note that the adjusted model (9) is different from the full factorial design of the (general) model (3). As the research goal of this section focuses on an aggregated level, all bivariate functions between the covariates DTIME, YDAY, OCOV, DCOV, and SDI are omitted. Not all combinations of continuous covariates are included, as the adjustment intends to answer the following questions:

Q1: Does the impact of COVID-19 on passenger demand change over time, i.e., is it different from one COVID-19 wave to another?

Q2: Does the impact of COVID-19 on passenger price elasticity change over time, i.e., is it different from one COVID-19 wave to another?

Q3: Do passengers book more spontaneously, i.e., closer to departure than pre-COVID-19 times?

The two functions $f_3(\ \text{BYDAY}_{i,t})$ and $f_{p,3}(p_{i,t},\ \text{BYDAY}_{i,t})$ are added to ensure that the impact of the selling-date-index (SDI) on passenger demand and price elasticity may not be affected by a booking seasonality.

Data Adjustments:

To ensure that the estimations for the departure date seasonality are unbiased, the results of "Estimation results" section depend on data where the entire booking period is observable for every flight. Suppose data for flights with an incomplete booking period is considered. In that case, demand estimates for future departure months can be lower, which may give a wrong impression of how demand changes during the departure year.

The models' demand predictions using post-COVID-19 data no longer apply to the market environment of COVID-19 times. As the models' ability to react to recent changes in previous selling dates depends on the input data, the data scope changes from a departure-date view to a selling-date view. The departure-date view (the dotted area within the top graph of Fig. 6) defines the data history of flights with complete selling-date history. The selling-date view (dotted area of the bottom graph of Fig. 6) describes the data set, where every selling date contains the entire (future) departure-date history. Assuming today's estimation date is 7/11/21, Fig. 6 shows that the data for departure date 7/11/22 is not available for the departure-date view until the models' estimation date reaches 7/11/22, whereas the selling-date view includes already all future fights until 7/11/22. Therefore, the benefit of having more up-to-date data and an accurate booking-behaviour representation (as captured by the functions $f_3(\ \text{BYDAY}_{i,t}), f_{p,3}(p_{i,t},\ \text{BYDAY}_{i,t}), f_4(\ \text{SDI}_{i,t}), f_{p,4}(p_{i,t},\ \text{SDI}_{i,t})$, and $f_{t,5}(t,\ \text{SDI}_{i,t})$) outweighs the risk of having a biased seasonality estimate for departure dates.

Results:

To answer the questions Q1, Q2, and Q3, the exp() is applied to both sides of the adjusted equation of model (9), which gives

$$\begin{aligned}&\lambda(\mathbf{x}_{i,t},t)^{\text{adj}} = \lambda(\mathbf{x}_{i,t},t)\\ &\times \underbrace{\exp\left(f_3(\ \text{BYDAY}_{i,t}) + f_4(\ \text{SDI}_{i,t}) + f_5(\ \text{OCOV}_{i,t}) + f_6(\ \text{DCOV}_{i,t})\right)}_{\text{Q1}^f}\\ &\times \underbrace{\exp\left(f_{p,3}(p_{i,t},\ \text{BYDAY}_{i,t}) + f_{p,4}(p_{i,t},\ \text{SDI}_{i,t}) + f_{p,5}(p_{i,t},\ \text{OCOV}_{i,t}) + f_{p,6}(p_{i,t},\ \text{DCOV}_{i,t})\right)}_{\text{Q2}^f}\\ &\times \underbrace{\exp\left(f_{t,5}(t,\ \text{SDI}_{i,t})\right)}_{\text{Q3}^f}.\end{aligned} \tag{10}$$

The underlined elements Q1^f, Q2^f, and Q3^f decrease or increase the unadjusted demand model (3), i.e.,

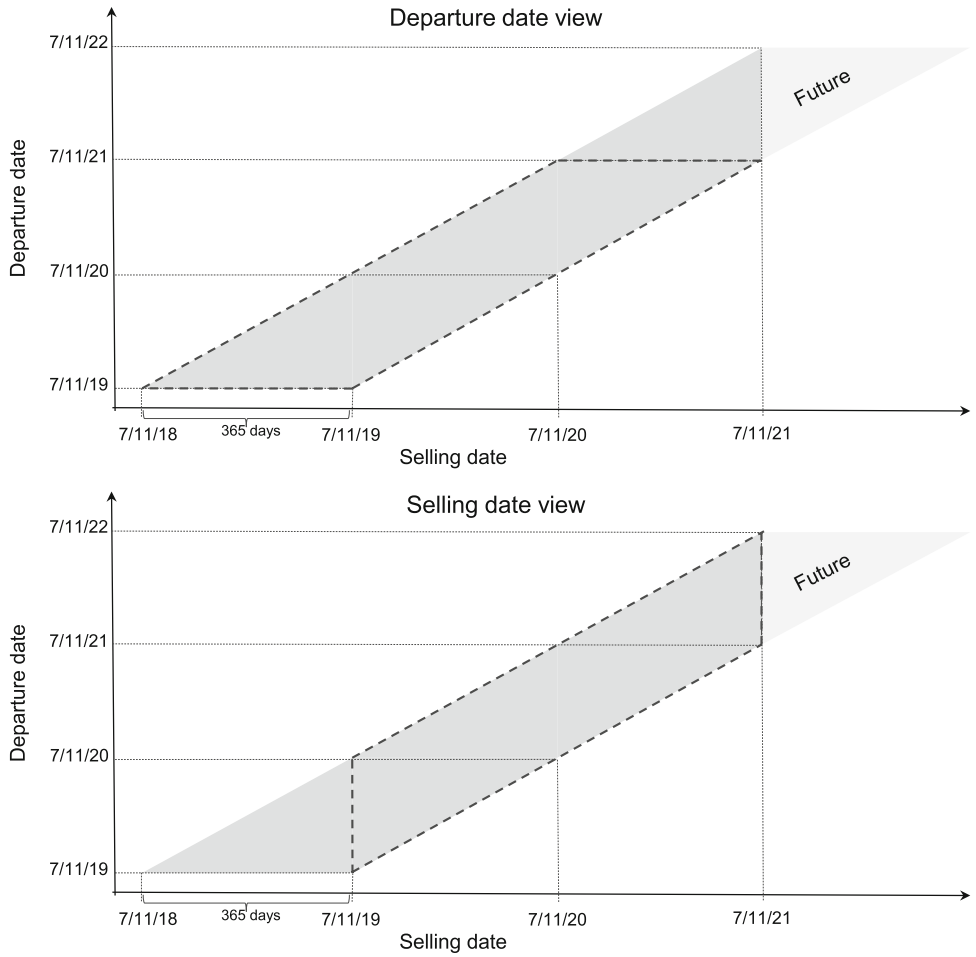

Fig. 6 Assuming today's estimation date is 7/11/21, the top graph describes the available data history for the departure date view. The departure dates range from 7/11/18 until 7/11/19, each with a 365-day selling date history. The dotted area of the bottom graph describes the data for the selling date view, where each selling date includes the booking history of past and future departure dates

$\log\left(\lambda(\mathbf{x}_{i,t}, t)\right)$ by a factor that depends on the additional covariates BYDAY, SDI, OCOV, and DCOV. Figure 7 shows how the factor $Q1^f$ changes the demand over the selling dates ranging from 2019-02-01 to 2021-04-11. As for the model (3), we segment the data by DDAY and P2P. Every line shows the $Q1^f$ estimate for a specific DDAY and P2P value. To answer the research question Q1, a steep drop in demand starting 2020-03-01, shortly before the first wave of COVID-19, is observed for every country. For some countries, specifically DE and GB, there is an increase in demand during the summer months between 2020-05-01 and 2020-09-01. For GB, we can observe a demand increase during the winter period. Therefore, depending on regulations and restrictions, every country reacts differently, highlighting the importance of capturing these effects within the demand model.

Figure 8 describes how the factor $\frac{\partial \log(Q2^f)}{\partial p_{i,t}}$, i.e., the price derivative of the logarithm of the factor $Q2^f$ changes the price elasticity over the selling dates ranging from 2019-02-01 to 2021-04-1. Suppose the adjusted demand model is used to derive optimal price values described in "Dynamic pricing" section. In that case, the factor appears within the denominator of the Eq. (8) and makes the profit margin depend on the additional covariates BYDAY, SDI, OCOV, and DCOV. The graph shows no significant changes in price elasticity, i.e., there is no visible trend and no change of price elasticity during the periods of first wave 2020-03-01 to 2021-05-01 (first wave) and 2020-08-01 and 2020-10-01 (second wave) implying that there is no connection to the number of new cases of COVID-19. Particularly for the countries DE and GB that show an increase in demand during the summer months between 2020-05-01 and 2020-09-01, no visible change in price elasticity is observed. Therefore, there is no evidence that the passengers' price elasticity has changed over time between the two waves of COVID-19. Moreover, these results imply that travel will likely not recover by offering cheaper tickets but by conditions that ensure travel safety.

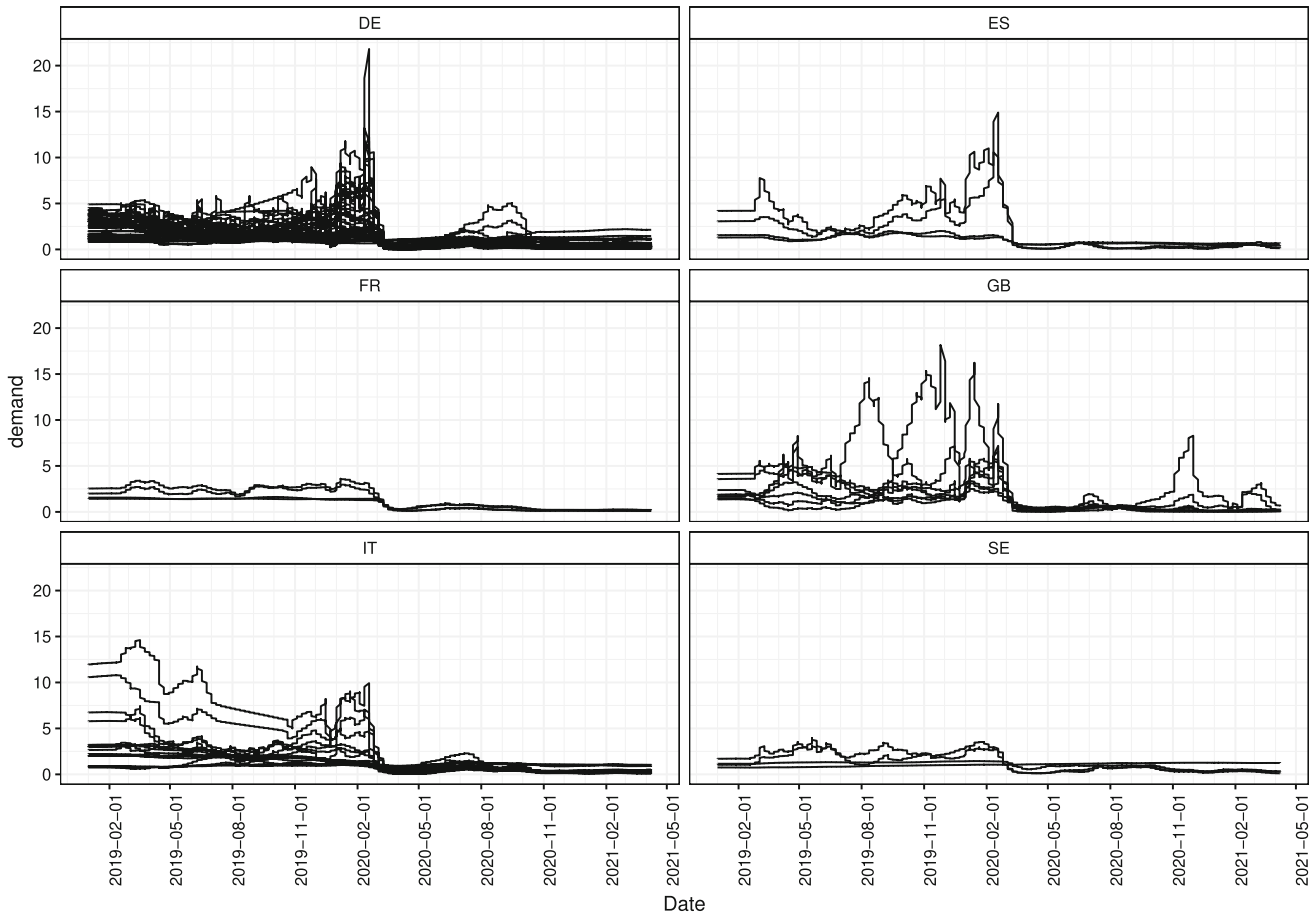

Fig. 7 For the countries DE, ES, FR, GB, IT, and SE, every line corresponds to an estimate of the factor $Q1^f$ from the adjusted model (3) for a specific DDAY and P2P value for selling dates ranging from 2019-02-01 to 2021-04-11

Finally, Fig. 9 describes the change in the booking behaviour over a 100-day booking period before departure from January 2021 to April 2021 for DE. The countries' ES, FR, GB, IT, and SE figures are in Appendix 7. Every graph shows that the booking behaviour of passengers has drastically changed for every country since the beginning of 2020. Whereas passenger demand steadily increased towards the day of departure, the booking curve is flat from 2020 until the end of the observed data range of April 2021. With the observations for 7 where a demand increase is observed for a certain period during the COVID-19 pandemic, airlines can no longer assume that passengers booking behaviour follows pre-COVID-19 patterns. Passenger demand arrives not necessarily spontaneously, with a booking curve only increasing shortly before departure and otherwise flat but sporadically throughout the booking period. This effect may be emphasised by the airlines' offering cheap tickets together with a waiver of cancellation and rebooking constraints to counter the increased uncertainty of passengers.

Conclusion

This paper introduces an innovative demand model that allows airline managers to deploy a controllable and interpretable pricing function to support the decision-making process of their revenue management department. The proposed method fulfills many important requirements of analysts and managers to have a demand estimation and pricing method, which is

flexible	as there is no need to pre-define a functional form, the method can be applied at scale (to various markets and conditions),
dynamic	as it captures differences in the customer's willingness to pay across various dimensions, ensuring optimal pricing policies,

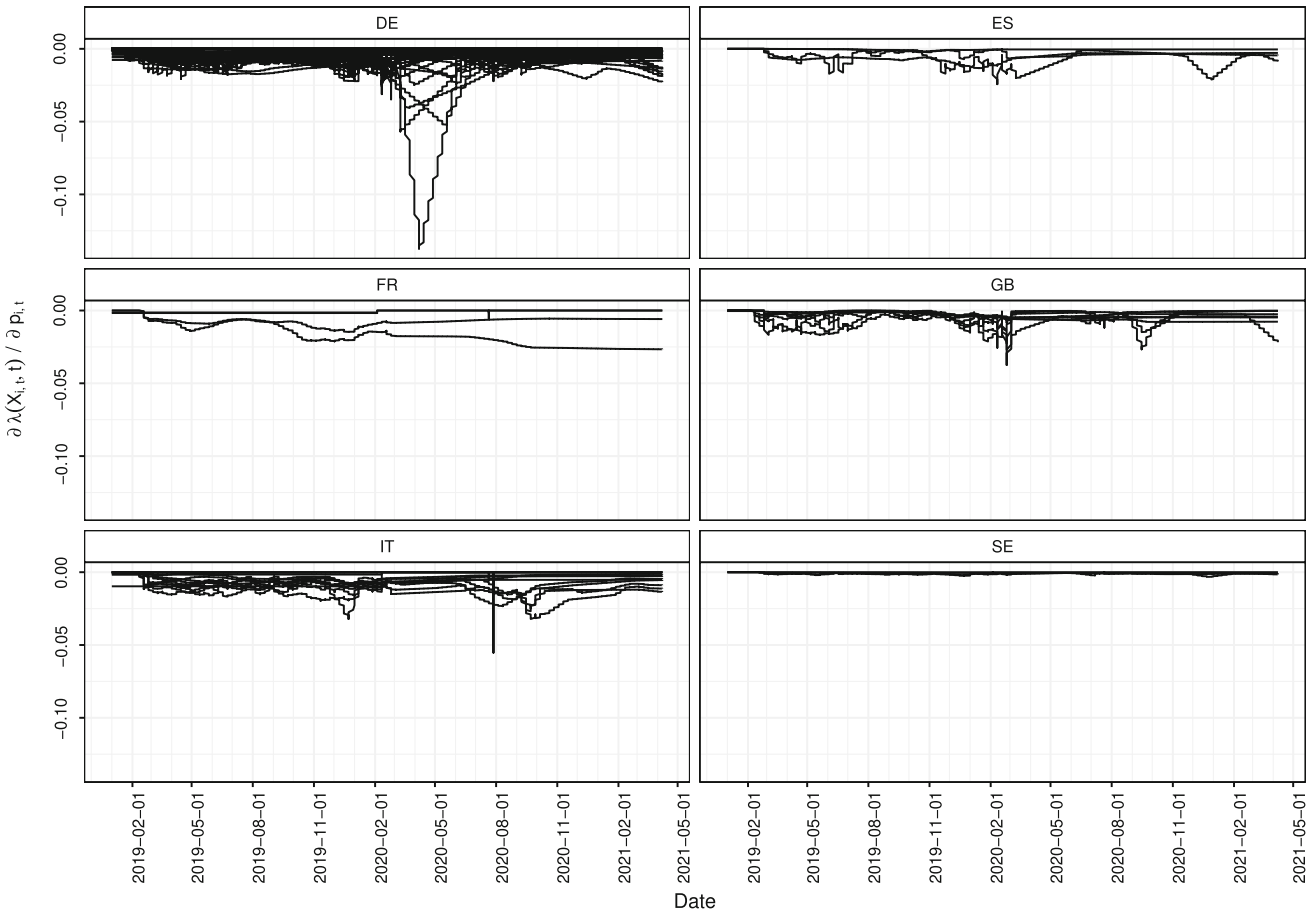

Fig. 8 For the countries DE, ES, FR, GB, IT, and SE, every line corresponds to an estimate of the factor $Q2^f$ from the adjusted model (3) for a specific DDAY and P2P value for selling dates ranging from 2019-02-01 to 2021-04-11

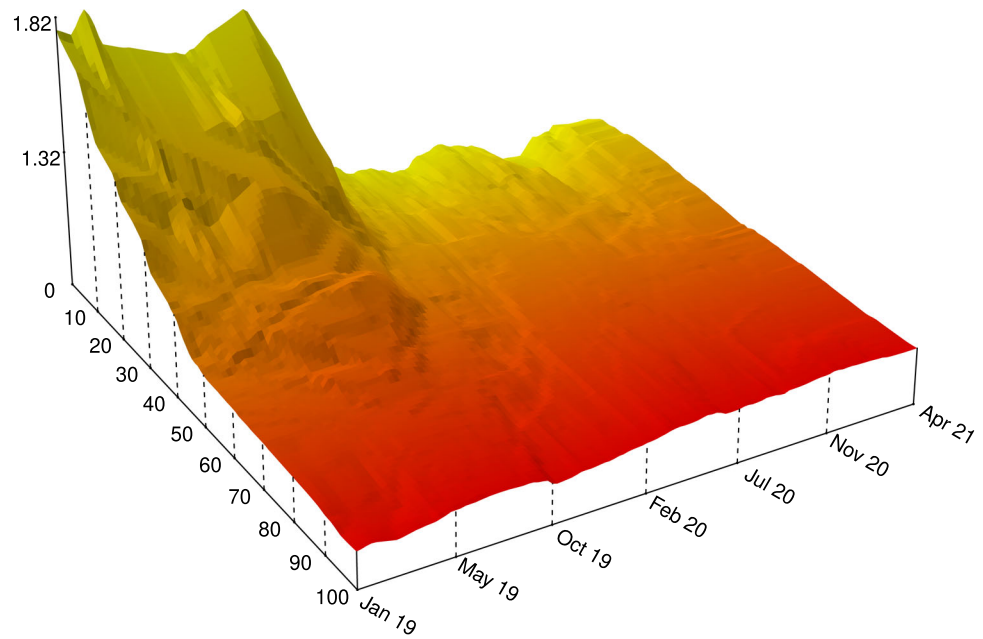

Fig. 9 For the country DE, the graph shows how the factor $Q3^f$ changes for different days to departure, ranging from 100 days pre-departure to the day of departure and over the selling dates from January 2019 to April 2021

easy to implement and computationally cheap	because the method offers a closed-form solution to the discrete and continuous pricing problem that determines the optimal price as the sum of costs and profit margin
easily to adopt	as most airlines organize their revenue management departments by separating pricing analysts (in control of the optimal profit margin) and steering analysts (in control of optimal 'costs', i.e., the bidprice)
considers of price-endogeneity	since the proposed instrumental variable is readily available in practical applications.

To achieve this, the proposed method extends the class of generalized additive models by combining smoothing spline ANOVA interaction components and monotonicity constraints, which shows superior forecasting performance if compared to other demand estimation techniques.

To validate the effectiveness of our approach, this paper shows practitioners the model's potential to significantly increase the revenue (+1.64% to +8.44%) and margin (+11.08% to +36.39%) but also showcases the flexibility of our approach by adapting the model's structure to changing market conditions such as the COVID-19 pandemic, where various unique insights could be revealed such as (1) the evidence that the impact of COVID-19 on-demand changes over time, (2) No evidence exists that the passengers' price elasticity has changed, which implies that travel will likely not recover by offering cheaper tickets but by conditions that ensure travel safety, and (3) as demand has increased for a certain period during the COVID-19 pandemic, airlines can no longer assume that passengers booking behavior follows pre-COVID-19 patterns.

As the following steps, we recommend investigating whether possible dependencies among customer segments could improve prediction accuracy. For segmentation, one could examine model-based partitioning (e.g. Zeileis et al. 2008). On another note, we explicitly excluded bookings of fares with fewer restrictions than the lowest available fare. As such features imply upsell, considering upsell-related passenger behaviour may further improve the revenue gain from dynamic pricing.

Appendix 1: Penalized likelihood estimation approach

We approximate each of the unknown function $f_p(\cdot)$,$f_t(\cdot)$, and $f_k(\cdot)$ by a weighted sum of local P-spline (penalised B-spline) basis functions (e.g. Eilers and Marx 1996). For example, the representation of $f_k(\cdot)$ is represented by a B-spline basis function given by the column vectors $\mathbf{b}_{k,j}(\cdot), j = 1, \ldots m$. The $n \times m$ matrix of basis functions $\mathbf{b}_k(\cdot) = \left(\mathbf{b}_{k,1}(\cdot), \mathbf{b}_{k,2}(\cdot), \ldots, \mathbf{b}_{k,m}(\cdot)\right)$ is subsequently multiplied by a $m \times 1$ vector of weighting coefficients $\boldsymbol{\gamma}_k$. Therefore, function $f_k(\cdot)$ is approximated by $\mathbf{b}_k(\cdot)\boldsymbol{\gamma}_k$. The column dimension m depends on the number of knots and degree of the B-spline functions (see, e.g. Marsh and Marshall 1999, Ch. 8, p. 187). The bivariate functions $f_{p,t}(\cdot,\cdot)$,$f_{p,k\in I_2}(\cdot,\cdot)$, and $f_{t,k\in I_2}(\cdot,\cdot)$,$f_{\substack{k_1<k_2 \\ k_1,k_2\in I_2}}(\cdot,\cdot)$ are also replaced in this manner. For example, $f_{k_1,k_2}(\cdot,\cdot)$ is replaced by $\mathbf{b}_{k_1,k_2}(\cdot,\cdot)\boldsymbol{\gamma}_{k_1,k_2}$, where the matrix of basis functions $\mathbf{b}_{k_1,k_2}(\cdot,\cdot)$ is built from their univariate marginal basis terms as $\mathbf{b}_{k_1,k_2}(\cdot,\cdot) = \mathbf{b}_{k_1}(\cdot) \otimes \mathbf{b}_{k_2}(\cdot)$. The Kronecker product $\otimes$ is calculated in a row-wise fashion.

Estimating the parameters in Eq. (3), requires identifiability constraints on the spline representations of the functions. Following Hastie and Tibshirani (1987) and Wood (2017), we require that the univariate functions $f_p(\cdot)$,$f_t(\cdot)$, and $f_k(\cdot)$ integrate out to zero. For the bivariate functions $f_{t,k\in I_2}(\cdot,\cdot)$ and $f_{\substack{k_1<k_2 \\ k_1,k_2\in I_2}}(\cdot,\cdot)$, we follow Lee and Durbán (2011), by applying the mixed model framework for smoothing. Lee and Durbán (2011) prove that the imposed constraints are equal to a classical factorial design. For the functions $f_{p,t}(\cdot,\cdot)$ and $f_{p,k\in I_2}(\cdot,\cdot)$, we exclude the first column of each marginal B-spline basis to achieve identifiability. For example, $f_{p,t}(\cdot,\cdot)$ is replaced by $\mathbf{b}_{p,t}(\cdot,\cdot)\boldsymbol{\gamma}_{p,t}$, where the matrix of basis functions $\mathbf{b}_{p,t}(\cdot,\cdot)$ is built from $\mathbf{b}_{p,t}(\cdot,\cdot) = \left(\mathbf{b}_{p,2}(\cdot), \ldots, \mathbf{b}_{p,m_p}(\cdot)\right) \otimes \left(\mathbf{b}_{t,2}(\cdot), \ldots, \mathbf{b}_{t,m_t}(\cdot)\right)$.

Having achieved identifiability, we compute parameter values by penalised maximum likelihood estimation. The penalty balances model flexibility and parsimony. The parameters of model (3) are given by $\boldsymbol{\theta} = (\boldsymbol{\beta}, \boldsymbol{\gamma})^T$. Here, $\boldsymbol{\beta} = \left(\beta_0, \boldsymbol{\beta}_1, \ldots, \boldsymbol{\beta}_{p,I_1}\right)^T$ concerns parametric covariates and the coefficient vector for the unknown functions is $\boldsymbol{\gamma} = \left(\boldsymbol{\gamma}_p, \boldsymbol{\gamma}_t, \boldsymbol{\gamma}_1, \ldots, \boldsymbol{\gamma}_{I_2}, \boldsymbol{\gamma}_{p,t}, \boldsymbol{\gamma}_{p,1}, \ldots, \boldsymbol{\gamma}_{p,I_2}, \boldsymbol{\gamma}_{t,1}, \ldots, \boldsymbol{\gamma}_{t,I_2}, \boldsymbol{\gamma}_{1,2}, \ldots, \boldsymbol{\gamma}_{I_2-1,I_2}\right)^T$.

This creates a feasible semi-parametric model, employing a high-dimensional basis and smoothed by imposing a penalty on $\boldsymbol{\gamma}$. The optimal values of the smoothing parameters are selected using the Bayesian

Information Criterion (BIC) (see also Claeskens and Hjort 2008, pp. 100–102).

The (unpenalized) log-likelihood $\ell(\boldsymbol{\theta})$ arising from Eqs. (1) and (2) is

$$\ell(\boldsymbol{\theta}) = \sum_{i=1}^{M} \sum_{t=t_i^{\text{close}}}^{t_i^{\text{open}}} y_{i,t} \log\left(\lambda(\mathbf{b}_{i,t}, t; \boldsymbol{\theta})\right) - \lambda(\mathbf{b}_{i,t}, t; \boldsymbol{\theta}), \qquad (11)$$

where the intensity $\lambda(\mathbf{x}_{i,t}, t; \boldsymbol{\theta})$ in Eq. (3) is written as a function of the covariates and the model parameters.

We maximize Eq. (11) with an additive penalty to regulate the degree of smoothness for every function of (3). The structure of (11) allows us to analytically calculate the first and second-order derivatives. Thereby, the derivatives are quickly evaluated and maximizing the likelihood proves straightforward by quasi Newton-Methods, such as the Broyden-Fletcher-Goldfarb-Shanno algorithm (e.g. Broyden 1970). The penalization is based on the ideas of Eilers and Marx (1996). We impose a penalty on the coefficients relating to all functional effects that define the demand model (3). We use linear B-splines for the marginals that concern $p_{i,t}$ and take quadratic B-splines otherwise. For the functions that have no shape constraint, i.e., $f_t, f_k, f_{t,k}, f_{k_1,k_2},\ k, k_1, k_2 \in I_2, k_1 < k_2$, we penalize neighbouring coefficients of second order.

For example, let $\mathbf{b}_t(\,t)$ be the quadratic B-spline bases for the main effect $f_t(t)$ with column dimension m_t and $\boldsymbol{\gamma}_t$ as the vector of weights. By penalizing second order differences, i.e., $\Delta^2\gamma_{t,l} = \gamma_{t,l} - 2\gamma_{t,l-1} + \gamma_{t,l-2}, l = m_t, \ldots, 3$. With the $(m_t - 2) \times m_t$ matrix

$$\mathbf{P}_t = \begin{bmatrix} 1 & -2 & 1 & 0 & \ldots & 0 \\ 0 & 1 & -2 & 1 & \ldots & 0 \\ \vdots & \vdots & \vdots & \vdots & \ddots & \vdots \\ 0 & 0 & 0 & 0 & \ldots & 1 \end{bmatrix}, \qquad (12)$$

the quadratic penalty for $f_t(t)$ is defined by $\boldsymbol{\gamma}_t^T \mathbf{S}_t \boldsymbol{\gamma}_t$, where $\mathbf{S}_t = \mathbf{P}_t^T \mathbf{P}_t$. Two penalty matrices $\mathbf{S}$ exist for bivariate effects, one for each dimension.

For the constrained functions $f_p, f_{p,t}$ and $f_{p,k}, k \in I_2$, we follow Pya (2010), who discusses uni- and bi-variate as well as single and double constraint functions. However, building the bivariate functions $f_{p,t}$ and $f_{p,k}, k \in I_2$ without the intercept values requires some adjustments. The first concerns the function $f_{p,t}$, which has a double monotonicity constraint. Here, we remove the first row and column vector from the matrices $\boldsymbol{\Sigma}_j, j = 1, 2$ (Pya 2010, p. 58). For the functions $f_{p,k}, k \in I_2$ with a monotonicity constraint along the first dimension $p_{i,t}$, we remove the first row and column vector of $\boldsymbol{\Sigma}_1$ and $\mathbf{I}_2$ (Pya 2010, p. 58). Secondly, for every bivariate function with monotonicity constraint, the penalty matrix $\mathbf{S}_j = \mathbf{P}_j^T \mathbf{P}_j, j \in \{1, 2\}$ is built from $\mathbf{P}_j$ without the first diagonal block element $\mathbf{P}_{uj}$ (Pya 2010, p. 60). The penalty matrix adjustments for f_{k_1,k_2} are discussed by Lee and Durbán (2011).

The penalised likelihood $\ell_p(...)$ is defined by the unpenalised version (11) plus the sum of the weighted quadratic penalties. Thus, for every function of model (3), the penalty matrix $\mathbf{S}$ is multiplied by a weighting factor ρ. For example, the weighted penalty term for $f_t(t)$ is defined by $\rho_t \boldsymbol{\gamma}_t^T \mathbf{S}_t \boldsymbol{\gamma}_t$. Collecting all weighted penalty matrices for every function finally leads to the expression:

$$\begin{aligned} \ell_p(\boldsymbol{\theta}, \boldsymbol{\rho}) = \ell(\boldsymbol{\theta}) &+ \rho_p \boldsymbol{\gamma}_p^T \mathbf{S}_p \boldsymbol{\gamma}_p \\ &+ \boldsymbol{\gamma}_{p,t}^T \left(\rho_{p,t,1} \mathbf{S}_{p,t,1} + \rho_{p,t,2} \mathbf{S}_{p,t,2}\right) \boldsymbol{\gamma}_{p,t} \\ &+ \sum_{k \in I_2} \boldsymbol{\gamma}_{p,k}^T \left(\rho_{p,k,1} \mathbf{S}_{p,k,1} + \rho_{p,k,2} \mathbf{S}_{p,k,2}\right) \boldsymbol{\gamma}_{p,k} \\ &+ \rho_t \boldsymbol{\gamma}_t^T \mathbf{S}_t \boldsymbol{\gamma}_t + \sum_{k \in I_2} \rho_k \boldsymbol{\gamma}_k^T \mathbf{S}_k \boldsymbol{\gamma}_k \\ &+ \sum_{k \in I_2} \boldsymbol{\gamma}_{t,k}^T \left(\rho_{t,k,1} \mathbf{S}_{t,k,1} + \rho_{t,k,2} \mathbf{S}_{t,k,2}\right) \boldsymbol{\gamma}_{t,k} \\ &+ \sum_{k_1 < k_2 \atop k_1, k_2 \in I_2} \boldsymbol{\gamma}_{k_1,k_2}^T \left(\rho_{k_1,k_2,1} \mathbf{S}_{k_1,k_2,1} + \rho_{k_1,k_2,2} \mathbf{S}_{k_1,k_2,2}\right) \boldsymbol{\gamma}_{k_1,k_2}, \end{aligned} \qquad (13)$$

where $\boldsymbol{\rho} = \left(\rho_p, \boldsymbol{\rho}_{p,t}, \boldsymbol{\rho}_{p,1}, \ldots, \boldsymbol{\rho}_{p,I_2}, \rho_t, \rho_1, \ldots, \rho_{I_2}, \boldsymbol{\rho}_{t,1}, \ldots, \boldsymbol{\rho}_{t,I_2}, \boldsymbol{\rho}_{1,2}, \ldots, \boldsymbol{\rho}_{I_2-1,I_2}\right)^T$ refers to the vector of penalty

parameters, weighting the quadratic penalties. Penalty parameters in bold correspond to column vectors. The first row gives the penalty of the first and the second row for the second dimension. For $\boldsymbol{\rho} = 0$, one obtains unpenalized estimations.

The penalty parameters are selected using the Bayesian Information Criterion defined through

$$BIC_\gamma(\boldsymbol{\rho}) = -2\ell_p(\boldsymbol{\theta}, \boldsymbol{\rho}) + \gamma \log(n)\ \mathrm{df}\ (\boldsymbol{\rho}), \tag{14}$$

where n is the number of observations ($\approx$ number of flights multiplied by the number of considered days to departure) and γ inflates the influence of df to increase the smoothness of the fit. The model degree of freedom df $(\boldsymbol{\rho})$ can be calculated through Fisher Matrices. Thus, let $F(\boldsymbol{\theta}, \boldsymbol{\rho})$ denote the penalized Fisher matrix, i.e.

$$F(\boldsymbol{\theta}, \boldsymbol{\rho}) = E\left(-\frac{\partial \ell_p(\boldsymbol{\theta}, \boldsymbol{\rho})}{\partial \boldsymbol{\theta} \partial \boldsymbol{\theta}^T}\right). \tag{15}$$

Then, the model degree can be approximated as

$$\mathrm{df}\ (\boldsymbol{\rho}) = \ \mathrm{trace}\ \{F^{-1}(\widehat{\boldsymbol{\theta}}, \boldsymbol{\rho}) F(\widehat{\boldsymbol{\theta}}, \boldsymbol{\rho} = 0)\},$$

see e.g. Krivobokova and Kauermann (2007). To estimate (5), we first maximise (13) for $\boldsymbol{\rho} = 0$. Secondly, given the estimate $\widehat{\boldsymbol{\theta}}$, we estimate $\boldsymbol{\rho}$ by minimising $BIC_\gamma(\boldsymbol{\rho})$. The corresponding estimate $\widehat{\boldsymbol{\rho}}$ is subsequently used to maximize (13) once more. We alternate the maximisation of (13) and minimisation of $BIC_\gamma(\boldsymbol{\rho})$ until $\left\|\frac{\partial BIC_\gamma(\boldsymbol{\rho})}{\partial \boldsymbol{\rho}}\right\|$, as calculated after the maximisation of (13), falls below a fixed threshold $\epsilon = 10^{-4}$.

Appendix 2: Two-staged estimation by residual inclusion

Treating price as an exogenous variable in a consumer demand model can lead to biased estimates of price elasticity; see discussions in Davidson and MacKinnon (1999, 1993), Wooldridge (2002), Petrin and Train (2010) and references therein. For example, Mumbower et al. (2014) show the importance of controlling for price endogeneity in a linear model for flight bookings using a two-stage least squares linear regression estimator, whereas Lurkin et al. (2017) do so for a choice model. For generalized nonlinear models, Marra and Radice (2011) suggest an extension of such two-stage estimators, similar to the control function approach of Petrin and Train (2010). We follow these authors and first build a nonlinear model for price based on an instrumental variable, and then include the price residual as a covariate in our model of passenger demand. To do so, we model the logarithm of prices at the daily and flight levels as

$$\begin{aligned}\log(p_{i,t}) =& \theta_0 + \theta_1\ \mathrm{IV}_{i,t} + \sum_{k \in I_1} \sum_{j \in J_k} \mathbf{1}_{\{x_{k,i,t}=j\}} \theta_{k,j} \\ &+ s_t(t) + \sum_{k \in I_2} s_k\left(z_{k,i,t}\right) + u_{i,t} \\ =& \eta_{i,t} + u_{i,t},\end{aligned} \tag{16}$$

where $u_{i,t} \sim N(0, \sigma^2)\ \forall\ i, t$. The effects of t and $z_{k,i,t}, k \in I_2$ are captured by unknown smooth functions $s_t()$ and $s_k(), k \in I_2$ modelled by penalized splines, while $\mathrm{IV}_{i,t}$ is an instrumental variable.

Mumbower et al. (2014) discusses possible choices for IV and suitable candidates. Li et al. (2014) describes that almost all of these choices are invalid as the researcher needs to observe both the IV and booking data at the same level of aggregation to control for price endogeneity effectively. Supply shifters—for example, airport fees, transportation taxes and fuel costs—are constant over daily bookings. Hausman-style instruments at the firm level do not match a model at the market level. Stern-type instruments that measure competition and market share do not vary on the booking level. Last, IVs that impact marginal costs remain a feasible option. Similar to (Meyer et al. 2022), we use (the logarithm of) a variable that is popular in the revenue management literature called the 'bidprice' (Talluri and van Ryzin 2005, p. 31). The bidprice is a measure of the (marginal) cost of offering a seat, taking into account that it cannot be sold again. Crucially, it varies between bookings because the airline updates its assessment frequently. The bidprice is available for all flights in the database and all time points and for prediction purposes for flights that have yet to depart.

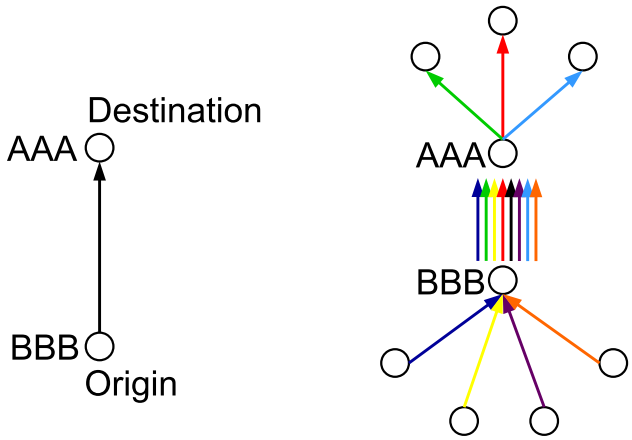

Fig. 10 Description of two Airline-network scenarios. On the left-hand side, the airline controls for capacity constraints only taking passenger demand from the origin (BBB) to the destination (AAA) into account. Low-cost carriers typically use this setup. On the right-hand side, the airline controls for the capacity constraint on the BBB to AAA route by taking all possible passenger demand streams coming from other origins than BBB (arrows going into BBB) to different destinations than AAA (arrows going out of AAA) into account. Network carriers typically use this setup

To ensure the validity of our choice, the IV needs to fulfil the properties of relevance and exogeneity (Guevara 2018). Whereas (strong) relevance can easily be demonstrated by the strong nonlinear dependence between the IV and the endogenous variable price, exogeneity needs to be addressed by a statistical (over-identification) test. Unfortunately, this test requires the availability of at least two instruments, so exogeneity can only be established definitely. From a qualitative perspective, the bidprice measures displacement cost, ensuring that revenue gain for the available airlines' network capacity is maximized. As pointed out by Li et al. (2014), the exogeneity (and hence the validity of the bid-price IV) means that a demand shock for flight i at the time to departure t (i.e. $\varepsilon_i(t) = Y_i(t) - \lambda(\mathbf{x}_{i,t}, t)$, where $Y_i(t) = N_i(t) - N_i(t-1)$) is uncorrelated with the IV. Figure 10 describes two possible revenue management setups, where an airline only controls displacement cost on the route level (left-hand side) or incorporates all potential demand streams into the displacement cost calculation (right-hand side). AirABC is a network carrier considering every demand stream when calculating the bidprice value. Therefore, the bidprice defines the distribution of network demand on the route level. In our study, the share of transfer passengers, i.e., passengers not travelling solely between BBB and AAA, is approximately 50%. Thus, the bid-price value is primarily determined by factors exogenous to the route under study. Hence, we conclude that the demand shock $\varepsilon_i(t)$ and the bidprice are uncorrelated.

After the parameters of the model (4) are estimated using maximum likelihood, the error

$$\begin{aligned}\xi_{i,t} =& p_{i,t} - \mathbb{E}\big(p_{i,t} \mid \text{IV}_{i,t}, z_{1,i,t}, \ldots, z_{I_2,i,t}\big)\\ =& p_{i,t} - \exp\big(\eta_{i,t} + \hat{\sigma}^2/2\big)\end{aligned}$$

is estimated for each flight and booking day combination, where the squared residual standard error is calculated as

$$\hat{\sigma}^2 = \frac{1}{n - \text{ df }(\widehat{\theta})} \sum_{i=1}^{M} \sum_{t=t_i^{\text{close}}}^{t_i^{\text{open}}} \widehat{u}_{i,t}^2, \tag{17}$$

The resulting residuals values are observations on the covariate $\hat{\xi}_{i,t}$, which is included in the demand model (3) as an additional regressor.

Appendix 3: Model adjustments for price data on booking level

The ticket price $p_{i,t}$ can change during booking day t, but covariates BDAY, DTIME, YDAY, and t are fixed. Therefore, the price is observed per booking, but BDAY, DTIME, YDAY, and t are given daily. The likelihood of model (5) is augmented to incorporate different resolution levels for the observations, specifically price variation on booking level. The augmentation aims to maintain the price information $p_{i,t}$ per booking.

Suppose three bookings are observed on a single day for model (5) with likelihood (11). In that case, we assume an aggregation level of $\frac{1}{3}$ day. To specify this here, let

$$\mathbf{x}_{i,t,l} = \big(\text{ BDAY}_{i,t}, p_{i,t,l}, \text{ DTIME}_{i,t}, \text{ YDAY}_{i,t}, t\big)$$

be the covariate vector for the lth booking observed t days to departure for flight i, where $l = 1, \ldots, \max(1, y_{i,t})$. On days without bookings of flight i (i.e. when $y_{i,t} = 0$), let $\mathbf{x}_{i,t,1}$ be the vector of covariate values, and set $y_{i,t,1} = 0$. Similarly, let $y_{i,t,l} = 1$ for $l = 1, \ldots, \max(1, y_{i,t})$ for days with observed bookings ($y_{i,t} \geq 1$). Then, the (unpenalized) log-likelihood is:

$$\begin{aligned}\ell(\boldsymbol{\theta}) = \sum_{i=1}^{M} \sum_{t=t_i^{\text{close}}}^{t_i^{\text{open}}} \sum_{l=1}^{\max(1,y_{i,t})} & y_{i,t,l} \log\Big(\lambda(\mathbf{x}_{i,t,l}, t; \boldsymbol{\theta})\Big)\\ & - \frac{\lambda(\mathbf{x}_{i,t,l}, t; \boldsymbol{\theta})}{\max(1, y_{i,t})}.\end{aligned} \tag{18}$$

The additional inner summation in Eq. (18) runs over all observed bookings ($y_{i,t,l} = 1$) during one booking day t and flight i. This summation drops out for days without bookings ($y_{i,t,l} = 0$).

Appendix 4: Benchmarking

We benchmark our approach against a heuristic, a parametric and a nonparametric model. As a representative heuristic, we select the model proposed by Weatherford and Pölt (2002) (WP). WP imputed the mean number of bookings as a demand estimate for days where the airline did not offer a fare. As a parametric approach, we select FCST of Fiig et al. (2014). This approach models demand depending on BDAY, DTIME, YDAY, t, and $p_{i,t}$. As a nonparametric approach, we select EM by Vulcano et al. (2012). EM requires price variation for all flights i and values of t. However, for the analysed data set, this is only sometimes given. So, instead of using the observed bookings with prices $p_{i,t}$, we calculate the average number of bookings for all observable prices. This logic imposes price variation for fixed values of t by dropping the flight index i. Therefore, EM predicts the average demand level per flight without considering season or departure time effects. Hence, we expect EM to perform best when demand does not depend on season or departure time and worse otherwise.

Table 6 lists the benchmarked models per represented family. The second column assesses model flexibility:

Table 6 Properties of forecasting models for benchmarking

Label	Flexibility	References
WP	Low	Weatherford and Pölt (2002)
FCST	Medium	Fiig et al. (2014)
EM	High	Vulcano et al. (2012)
Our model	High	Eqs. (4) and (5)

nonparametric models provide more flexibility than parametric models. WP is rated as less flexible than all alternatives, as it ignores the information contributed by the covariates BDAY, DTIME, YDAY, and t.

We measure the prediction error by K-fold cross-validation to quantify the forecasting accuracy. The smallest prediction error indicates the best demand estimate. We evaluate the prediction error per flight i. To that end, we aggregate observed bookings $y_{i,t}$ and demand estimates $\widehat{\lambda}(\mathbf{x}_{i,t}, t) \equiv \widehat{\lambda}_{i,t}$ over t: $y_i = \sum_{t=t_i^{\text{close}}}^{t_i^{\text{open}}} y_{i,t}$ and $\widehat{\lambda}_i = \sum_{t=t_i^{\text{close}}}^{t_i^{\text{open}}} \widehat{\lambda}_{i,t}$. To create K roughly equal-sized folds of data (indexed by $k \in \{1, \ldots, K\}$) from M flights ($K << M$), we randomly draw $m = \lfloor \frac{M}{K} \rfloor$ flights, K-times without replacement. Finally, for each competing model, the cross-validation estimate of the prediction error $\text{CV}\left(\widehat{\lambda}\right)$ is

$$\text{CV}\left(\widehat{\lambda}\right) = \frac{1}{K}\sum_{k=1}^{K}\frac{1}{M_k}\sum_{i=1}^{M_k} \text{L}\left(y_i, \widehat{\lambda}_i^{-k(i)}\right), \tag{19}$$

where prediction $\widehat{\lambda}_i^{-k(i)}$ is created by excluding the data of fold k. The loss $\text{L}\left(y_i, \widehat{\lambda}^{-k(i)}\right)$ results by forecasting $\widehat{\lambda}_i^{-k(i)}$ and observing y_i.

As loss functions $L(\cdot)$, we consider a selection of absolute and relative measures. We measure absolute deviations by the root mean squared error (RMSE) and the mean absolute deviation (MAD). Relative deviations are evaluated by the root mean squared logarithmic error (RMSLE) and the symmetric mean absolute percentage error (SMAPE), which are feasible if the target attains a value of zero (if no demand is observed). The definitions for RMSE, MAD, RMSLE, and SMAPE are

$$\text{RMSE} = \sum_{i=1}^{M}\left(y_i - \widehat{\lambda}_i^{-k(i)}\right)^2 \tag{20}$$

$$\text{MAD} = \sum_{i=1}^{M}\left|y_i - \widehat{\lambda}_i^{-k(i)}\right| \tag{21}$$

$$\text{RMSLE} = \sum_{i=1}^{M}\log\left(\frac{\widehat{\lambda}_i^{-k(i)}+1}{y_i+1}\right)^2 \tag{22}$$

$$\text{SMAPE} = \frac{\sum_{i=1}^{M}\left|y_i - \widehat{\lambda}_i^{-k(i)}\right|}{\sum_{i=1}^{M} y_i + \widehat{\lambda}_i^{-k(i)}} \tag{23}$$

Figure 11 reports the resulting average cross-validation estimates $\overline{\text{CV}}\left(\widehat{\lambda}\right)$ per benchmarked approach and sample size. Two P2P connections and seven departure days yield 14 combinations per OD. Thus, the average cross-validation estimate for prediction $\widehat{\lambda}$ is calculated as $\overline{\text{CV}}\left(\widehat{\lambda}\right) = \frac{1}{14}\sum_{j=1}^{14} \text{CV}_j$. Figure 11 shows that the two absolute measures tend to increase in the sample size, whereas the relative measures RMSLE and SMAPE decrease. Our approach ranges at the top independent of the sample size, even though FCST performs almost as well. The weak performance of EM originates from not considering seasonal or departure time dependencies but being dependent on aggregated data. The relative measures of RMSLE and SMAPE highlight the superior performance of our model. As Bartke (2014) point out, small observations result if disaggregated booking data is used for demand estimation. Therefore, the final judgment should focus on relative forecasting performance as quantified by RMSLE and SMAPE.

Appendix 5: Proof of the discrete pricing problem

Given a discrete set of price points $\Omega_p = \{p_1, \ldots, p_J\}$, the optimal price $p_{i,t}^{\star}$ (8) defines the lower boundary point of the subset $\Omega_p' \subset \Omega_p$ of prices that are profitable to be offered. To show that $p_{i,t}^{\star}$ defines the boundary point of the set Ω_p', every price below ($p_k < p_{i,t}^{\star}$) has to have a marginal revenue contribution that is smaller than $\pi_{i,t}$ (bid-price) and a price above or equal ($p_j \geq p_{i,t}^{\star}$) has to have a marginal revenue contribution that is greater than π.

Proof for simplicity all indices are dropped For $p_k < p^{\star}$:

$$\begin{aligned} &\lambda(p_k)r_k - \lambda(p_k)\pi < \lambda(p^{\star})r^{\star} - \lambda(p^{\star})\pi \\ &\iff \lambda(p_k)r_k - \lambda(p^{\star})r^{\star} - \pi\left(\lambda(p_k) - \lambda(p^{\star})\right) < 0 \\ &\iff \frac{\lambda(p_k)r_k - \lambda(p^{\star})r^{\star}}{\lambda(p_k) - \lambda(p^{\star})} < \pi \end{aligned} \tag{24}$$

For $p_j > p^{\star}$:

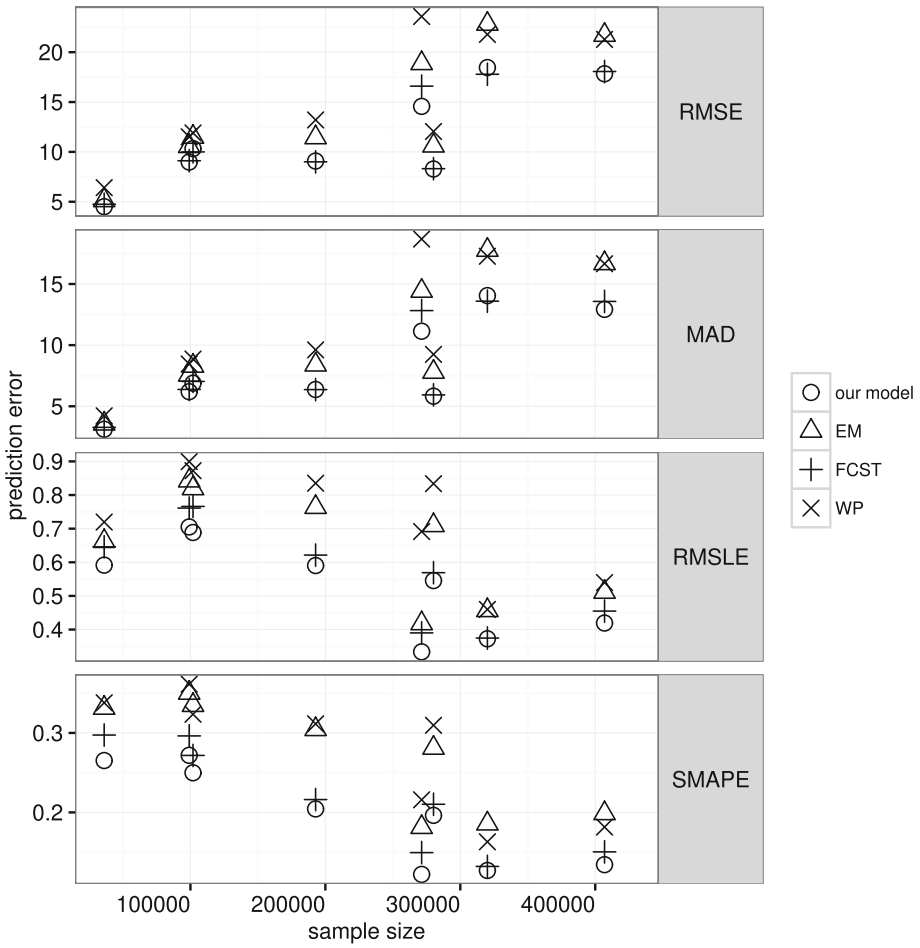

Fig. 11 Estimates of the average prediction error $\overline{\mathrm{CV}}(\widehat{\lambda})$ versus the ODs sample size calculated by the criteria RMSE (1st row), MAD (2nd row), RMSLE (3rd row), and SMAPE (4th row). The model with the lowest prediction error among all other models (our model, EM, FCST, and WP) has the best forecasting performance for every criterion

$$\begin{aligned} &\lambda(pj)r_j - \lambda(p_j)\pi < \lambda(p^\star)r^\star - \lambda(p^\star)\pi \\ &\iff \lambda(p_j)r_j - \lambda(p^\star)r^\star - \pi\big(\lambda(p_j) - \lambda(p^\star)\big) < 0 \\ &\iff \frac{\lambda(p^\star)r^\star - \lambda(p_j)r_j}{\lambda(p^\star) - \lambda(p_j)} > \pi \end{aligned} \tag{25}$$

We conclude that prices below the optimal price ($p_k < p^\star$) have a marginal revenue contribution smaller than the bidprice and are therefore not included in the offer-set Ω'_p. In contrast, prices equal to or greater than the optimal price $p^\star$ have a marginal revenue contribution greater than the bidprice and are therefore included in Ω'_p. Note that the first inequality of each case results as $p^\star$ is the optimal price that maximises (6).

Appendix 6: Calculation of the optimal continuous price

$$
\begin{aligned}
&\frac{\partial\Big(\lambda(\mathbf{x}_{i,t},t)(r_{i,t}-\pi_{i,t})\Big)}{\partial p_{i,t}} \stackrel{!}{=} 0\\
&\iff (\widehat{r}^{\star}_{i,t}-\pi_{i,t})\frac{\partial\lambda(\mathbf{x}_{i,t},t)}{\partial p_{i,t}}+\lambda(\mathbf{x}_{i,t},t)\frac{\partial(\widehat{r}^{\star}_{i,t}-\pi_{i,t})}{\partial p_{i,t}}=0\\
&\iff \Big(-\widehat{\alpha}_0+(1-\widehat{\alpha}_1)p^{\star}_{i,t}-\pi_{i,t}\Big)\frac{\partial\lambda(\mathbf{x}_{i,t},t)}{\partial p_{i,t}}\\
&\quad+\lambda(\mathbf{x}_{i,t},t)(1-\widehat{\alpha}_1)=0\\
&\iff \Big(-\widehat{\alpha}_0+(1-\widehat{\alpha}_1)p^{\star}_{i,t}-\pi_{i,t}\Big)\lambda(\mathbf{x}_{i,t},t)\frac{\partial\log\big(\lambda(\mathbf{x}_{i,t},t)\big)}{\partial p_{i,t}}\\
&\quad+\lambda(\mathbf{x}_{i,t},t)(1-\widehat{\alpha}_1)=0\\
&\iff \Big(-\widehat{\alpha}_0+(1-\widehat{\alpha}_1)p^{\star}_{i,t}-\pi_{i,t}\Big)\\
&\quad\left(\mathbf{1}_{2s}\widehat{\beta_{\xi}}+f'_p+f'_{p,t}(t)+\sum_{k\in I_2}f'_{p,k}(z_{k,i,t})\right)=-(1-\widehat{\alpha}_1)\\
&\iff -\frac{1-\widehat{\alpha}_1}{\mathbf{1}_{2s}\widehat{\beta_{\xi}}+f'_p+f'_{p,t}(t)+\sum_{k\in I_2}f'_{p,k}(z_{k,i,t})}\\
&\quad+\widehat{\alpha}_0+\pi_{i,t}=(1-\widehat{\alpha}_1)p^{\star}_{i,t}\\
&\iff -\frac{1}{\mathbf{1}_{2s}\widehat{\beta_{\xi}}+f'_p+f'_{p,t}(t)+\sum_{k\in I_2}f'_{p,k}(z_{k,i,t})}\\
&\quad+\frac{\widehat{\alpha}_0}{1-\widehat{\alpha}_1}+\frac{\pi_{i,t}}{1-\widehat{\alpha}_1}=p^{\star}_{i,t}
\end{aligned}
\tag{26}
$$

In line two, we use the fact that the estimated regression model (7) gives $\widehat{r}_{i,t}=-\widehat{\alpha}_0+(1-\widehat{\alpha}_1)p_{i,t}$. Thus, for $p_{i,t}=p^{\star}_{i,t}$ we get the corresponding revenue gain $\widehat{r}^{\star}_{i,t}$. The model for $\log\big(\lambda(\mathbf{x}_{i,t},t)\big)$ is defined by Eq. (3). Specifically, Eq. (5) describes the model applied to airline data. In line 5, we used the structure of the airline model, where f' corresponds to $\frac{\partial}{\partial p_{i,t}}f$.

Appendix 7: Supplementary plots

Figure 12 shows the offered price per departure time and three values of bidprice π for OD1-5 and OD7. Figure 13 shows how the factor Q3 of π changes for the countries ES, FR, GB, IT, and SE.

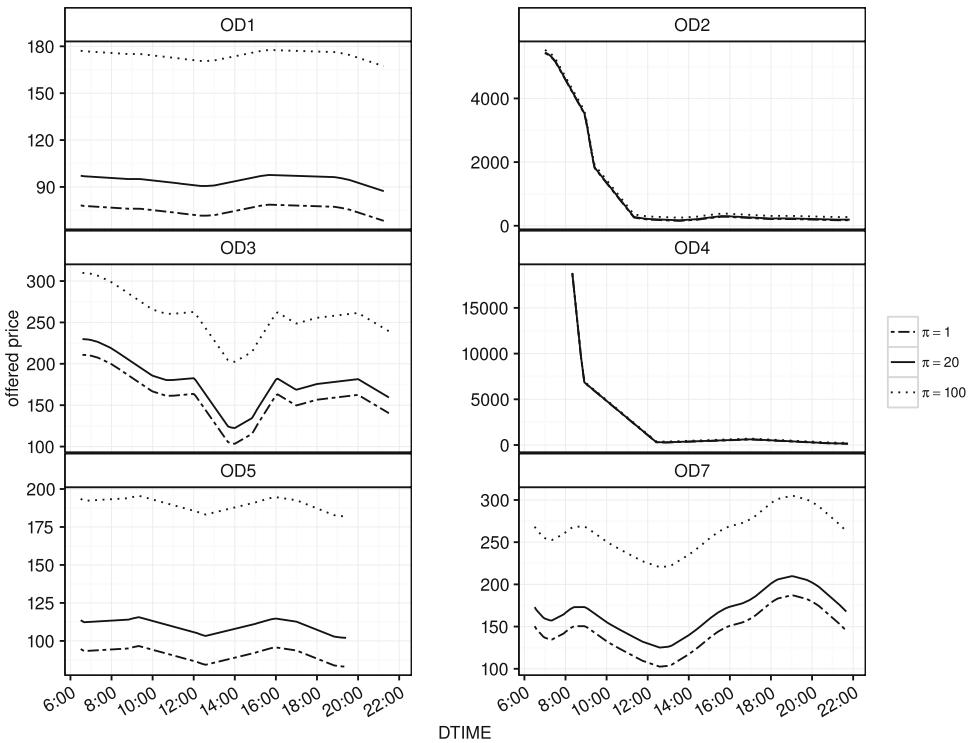

Fig. 12 Optimal price values for OD1-5 and OD7 at DDAY=Thursday

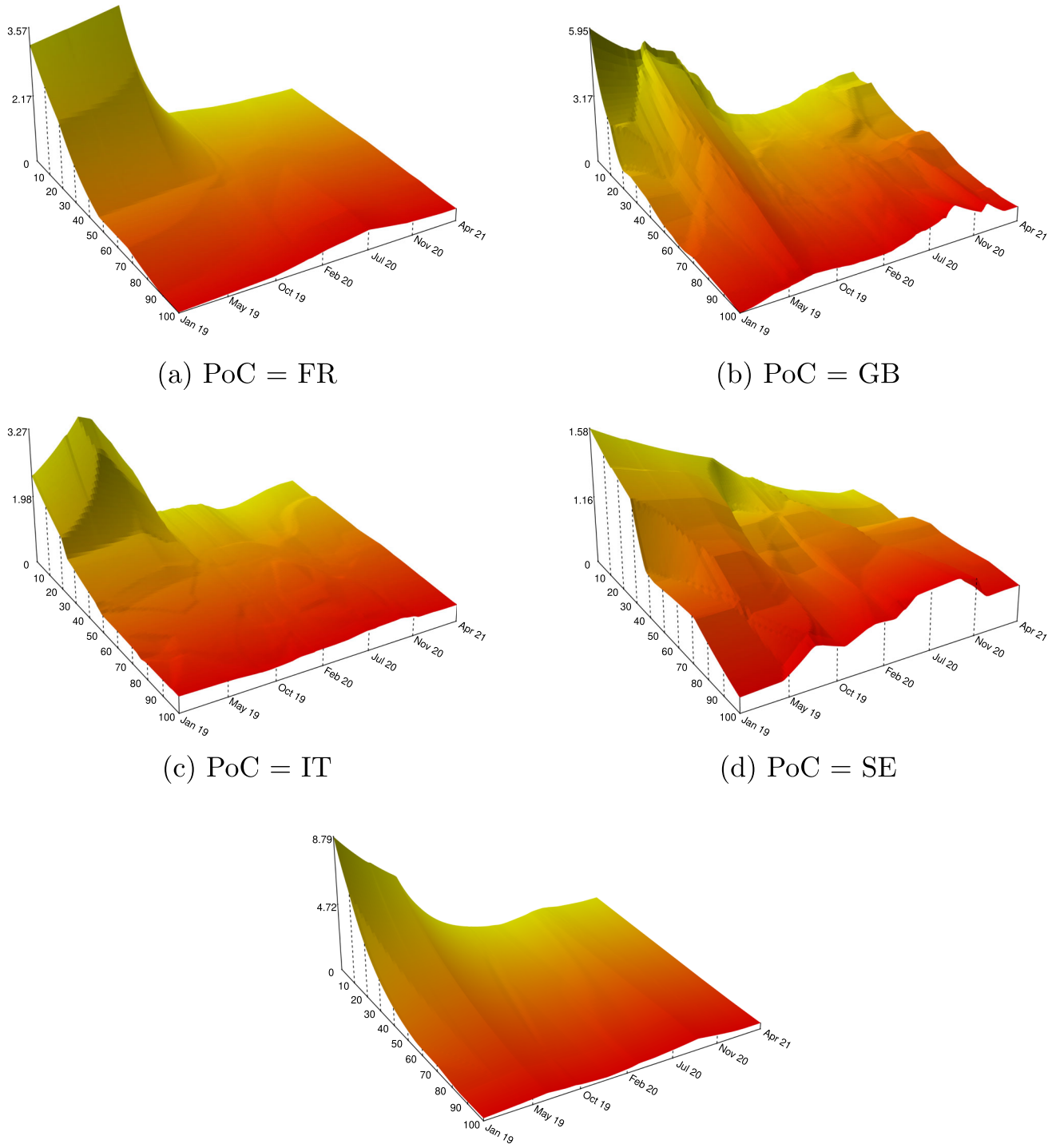

Fig. 13 For the countries ES, FR, GB, IT, and SE, the graph shows how the factor $Q3^f$ changes for different days to departure, ranging from 100 days pre-departure to the day of departure and over the selling dates from January 2019 to April 2021

Funding Open Access funding enabled and organized by Projekt DEAL.

Data availability As such features imply upsell, analyzing data about upsell-related passenger behavior could further enhance revenue gains from dynamic pricing.

References

Arandia, E. 2013. Spatial-temporal statistical modeling of treated drinking water usage. Ph.D. thesis, University of Cincinnati. http://etd.ohiolink.edu/rws_etd/document/get/ucin1377870978/inline

Avramidis, A.N. 2013. Learning in revenue management: Exploiting estimation of arrival rate and price response. http://www.personal.soton.ac.ukaa1w07/v35.pdf

Bartke, P. 2014. Demand estimation in airline revenue management. Ph.D. thesis, FU Berlin. http://www.diss.fu-berlin.de/diss/receive/FUDISS_thesis_000000096263?lang=en

Besbes, O., and A. Zeevi. 2009. Dynamic pricing without knowing the demand function: Risk bounds and near-optimal algorithms. *Operations Research* 57 (6): 1407–1420. https://doi.org/10.1287/opre.1080.0640.

Besbes, O., and A. Zeevi. 2015. On the (surprising) sufficiency of linear models for dynamic pricing with demand learning. *Management Science* 61 (4): 723–739. https://doi.org/10.1287/mnsc.2014.2031.

Bingemer, Stephan. 2018. Back to the future with IATA NDC? Critical turning points in the history of airline distribution. *Journal of Tourism Futures* 4 (3): 205–217.

Blundell, R., J.L. Horowitz, and M. Parey. 2012. Measuring the price responsiveness of gasoline demand: Economic shape restrictions and nonparametric demand estimation. *Quantitative Economics* 3 (1): 29–51. https://doi.org/10.3982/QE91.

Bonciolini, G. 2022. Automatic adjustment of dynamic pricing under turbulent market conditions. https://publications.agifors.org/documents/1-06%20Giacomo_bonciolini_Price%20Elasticity%20Monitor.pdf

Brezger, A., and W.J. Steiner. 2008. Monotonic regression based on Bayesian p-splines: An application to estimating price response functions from store-level scanner data. *Journal of Business Economics* 26 (1): 90–104.

Broyden, C.G. 1970. The convergence of a class of double-rank minimization algorithms 1. General considerations. *SIAM Journal on Applied Mathematics* 6 (1): 76–90.

Chen, Q.G., J. Stefanus, and I. Duenyas. 2014. Adaptive parametric and nonparametric multi-product pricing via self-adjusting controls. *Ross School of Business Paper*. https://doi.org/10.2139/ssrn.2533468.

Claeskens, G., and N.L. Hjort. 2008. *Model selection and model averaging. Cambridge series in statistical and probabilistic mathematics*. Cambridge: Cambridge University Press.

Dai, J., W. Ding, A. Kleywegt, X. Wang, and Y. Zhang. 2014. Choice based revenue management for parallel flights. http://ssrn.com/abstract=2404193

Davidson, R., and J.G. MacKinnon. 1993. *Estimation and inference in econometrics*, 1st ed. Oxford: Oxford University Press.

Davidson, R., and J.G. MacKinnon. 1999. *Econometric theory and methods*, 1st ed. Oxford: Oxford University Press.

de Boor, C. 1978. *A practical guide to splines*. Berlin: Springer.

den Boer, A.V. 2015. Dynamic pricing and learning: Historical origins, current research, and new directions. *Surveys in Operations Research and Management Science* 20 (1): 1–18.

Eilers, P.H.C., and B.D. Marx. 1996. Flexible smoothing with B-splines and penalties. *Statistical Science* 11: 89–121.

Farias, V.F., S. Jagabathula, and D. Shah. 2013. A nonparametric approach to modeling choice with limited data. *Management Science* 59 (2): 305–322. https://doi.org/10.1287/mnsc.1120.1610.

Fiig, T., U. Cholak, M. Gauchet, and B. Cany. 2015. What is the role of distribution in revenue management?—Past and future. *Journal of Revenue and Pricing Management* 14 (2): 127–133.

Fiig, T., R. Hardling, S. Pölt, and C. Hopperstad. 2014. Demand forecasting and measuring forecast accuracy. *Journal of Revenue and Pricing Management* 13 (6): 413–439.

Fiig, T., K. Isler, C. Hopperstad, and P. Belobaba. 2010. Optimization of mixed fare structures: Theory and applications. *Journal of Revenue and Pricing Management* 9: 152–170. https://doi.org/10.1057/rpm.2009.18.

Gu, C. 2002. Smoothing spline ANOVA models. In *IMA volumes in mathematics and its applications*. Berlin: Springer.

Guevara, C.A. 2018. Overidentification tests for the exogeneity of instruments in discrete choice models. *Transportation Research B* 114 (C): 241–253.

Hastie, T., and R. Tibshirani. 1987. Generalized additive models: Some applications. *Journal of the American Statistical Association* 82 (398): 371–386.

IATA. 2018. IATA dynamic offer creation. https://www.iata.org/whatwedo/airline-distribution/Documents/air-white-paper-dynamic-offer-creation.pdf. Accessed 19 June 2019

Keskin, N.B., and A. Zeevi. 2014. Dynamic pricing with an unknown demand model: Asymptotically optimal semi-myopic policies. *Operations Research* 62 (5): 1142–1167. https://doi.org/10.1287/opre.2014.1294.

Krivobokova, T., and G. Kauermann. 2007. A note on penalized spline smoothing with correlated errors. *Journal of the American Statistical Association* 102: 1328–1337.

Lee, D.-J., and M. Durbán. 2011. P-spline anova-type interaction models for spatio-temporal smoothing. *Statistical Model* 11 (1): 49–69. https://doi.org/10.1177/1471082X1001100104.

Leemis, L.M. 1991. Nonparametric estimation of the cumulative intensity function for a nonhomogeneous Poisson process. *Management Science* 37 (7): 886–900.

Li, J., N. Granados, and S. Netessine. 2014. Are consumers strategic? structural estimation from the air-travel industry. *Management Science* 60 (9): 2114–2137.

Lo, W.W.L., Y. Wan, and A. Zhang. 2015. Empirical estimation of price and income elasticities of air cargo demand: The case of Hong Kong. *Transportation Research A* 78: 309–324. https://doi.org/10.1016/j.tra.2015.05.014.

Lurkin, Virginie, Laurie A. Garrow, Matthew J. Higgins, Jeffrey P. Newman, and Michael Schyns. 2017. Accounting for price endogeneity in airline itinerary choice models: An application to

continental us markets. *Transportation Research A* 100: 228–246.
Marra, G., and R. Radice. 2011. A flexible instrumental variable approach. *Statistical Modelling* 11 (6): 581–603.
Marsh, D., and D.L. Marshall. 1999. *Applied geometry for computer graphics*, 1st ed. London: Springer.
Marx, B.D., M. Durban, and P.H.C. Eilers. 2016. Twenty years of p-splines. *Statistics, and Optimization, Operations Research* 39 (2): 149–186.
Meyer, Jan Felix, Göran. Kauermann, and Michael Stanley Smith. 2022. Interpretable modelling of retail demand and price elasticity for passenger flights using booking data. *Statistical Modelling*. https://doi.org/10.1177/1471082X221083343.
Mumbower, S., L.A. Garrow, and M.J. Higgins. 2014. Estimating flight-level price elasticities using online airline data: A first step toward integrating pricing, demand, and revenue optimization. *Transportation Research A* 66: 196–212.
Newman, J.P., L. Garrow, M. Ferguson, T.L. Jacobs, and H. Purnomo. 2014. Estimation of choice-based models using sales data from a single firm. *Manufacturing & Service Operations Management* 16 (2): 184–197.
OWID. 2021. Coronavirus source data. https://ourworldindata.org/coronavirus-source-data. Accessed 12 Apr 2021
Petrin, A., and K. Train. 2010. A control function approach to endogeneity in consumer choice models. *Journal of Marketing Research* 47: 3–13.
Pinheiro, Gatti, Thomas Fiig Giovanni, Michael D. Wittman, Michael Defoin-Platel, and Riccardo D. Jadanza. 2022. Demand change detection in airline revenue management. *Journal of Revenue and Pricing Management* 21 (6): 581–595. https://doi.org/10.1057/s41272-022-00385-8.
Pölt, S., J. Rauch, and K. Isler. 2018. Disentangling capacity control from price optimization. *Journal of Revenue and Pricing Management* 17: 48–62.
Pya, N. 2010. Additive models with shape constraints. Ph.D. thesis, University of Bath. http://opus.bath.ac.uk/27546/
Pya, N., and S.N. Wood. 2014. Shape constrained additive models. *Statistics and Computing* 25 (3): 543–559. https://doi.org/10.1007/s11222-013-9448-7.
Qiang, S., and M. Bayati. 2016. Dynamic pricing with demand covariates. https://doi.org/10.2139/ssrn.2765257
Sankaranarayanan, H.B., and J. Lalchandani. 2019. Smart omnichannel architecture for air travel applications using big data techniques. In *International conference on computer networks and communication technologies*, ed. S. Smys, J.I.-Z. Bestak, R. Chen, and I. Kotuliak, 661–669. Singapore: Springer.
Talluri, K.T., and G.J. van Ryzin. 2005. The theory and practice of revenue management. In *International Series in Operations Research & Management Science*. Berlin: Springer
Tutz, G., and F. Leitenstorfer. 2007. Generalized monotonic regression based on b-splines with an application to air pollution data. *Biostatistics* 8 (3): 654–673. https://doi.org/10.1093/biostatistics/kxl036.
Vinod, B. 2021. An approach to adaptive robust revenue management with continuous demand management in a COVID-19 era. *Journal of Revenue and Pricing Management* 20 (1): 10–14. https://doi.org/10.1057/s41272-020-00269-9.
Vulcano, G., G. van Ryzin, and W. Chaar. 2010. Choice-based revenue management: An empirical study of estimation and optimization. *Manufacturing & Service Operations Management* 12 (3): 371–392.
Vulcano, G., G. van Ryzin, and R. Ratliff. 2012. Estimating primary demand for substitutable products from sales transaction data. *Operations Research* 60 (2): 313–334.
Weatherford, L., and S. Pölt. 2002. Better unconstraining of airline demand data in revenue management systems for improved forecast accuracy and greater revenues. *Journal of Revenue and Pricing Management* 1: 234–254.
Wittman, M.D., and P.P. Belobaba. 2017. Personalization in airline revenue management—Heuristics for real-time adjustment of availability and fares. *Journal of Revenue and Pricing Management* 16 (4): 376–396. https://doi.org/10.1057/s41272-016-0002-z.
Wittman, M.D., and P.P. Belobaba. 2019. Dynamic pricing mechanisms for the airline industry: A definitional framework. *Journal of Revenue and Pricing Management* 18 (2): 100–106. https://doi.org/10.1057/s41272-018-00162-6.
Wood, S. 2017. *Generalized additive models: An introduction with R. CRC texts in statistical science*. Boca Raton: CRC Press.
Wooldridge, J. 2002. *Introductory econometrics: A modern approach*, 2nd ed. East Lansing: Michigan State University.
Wu, S., and A. Akbarov. 2012. Forecasting warranty claims for recently launched products. *Reliability Engineering & System Safety* 106: 160–164.
Xie, X., R. Verma, and C.K. Anderson. 2016. Demand growth in services: A discrete choice analysis of customer preferences and online selling. *Decision Sciences* 47 (3): 473–491. https://doi.org/10.1111/deci.12177.
Yeoman, I. 2021. Q. Can we manage demand in COVID-19 world? A. I don't know. *Journal of Revenue and Pricing Management* 20 (1): 1–2. https://doi.org/10.1057/s41272-021-00280-8.
Yeoman, Ian. 2022. Ukraine, price and inflation. *Journal of Revenue and Pricing Management* 21 (3): 253–254. https://doi.org/10.1057/s41272-022-00378-7.
Zeileis, A., T. Hothorn, and K. Hornik. 2008. Model-based recursive partitioning. *Journal of Computational and Graphical Statistics* 17 (2): 492–514.
Zhang, T., and S.C. Kou. 2010. Nonparametric inference of doubly stochastic Poisson process data via the kernel method. *The Annals of Applied Statistics* 4 (4): 1913–1941. https://doi.org/10.1214/10-AOAS352.